Fryer, P., Pearce, J. A., Stokking, L. B., et al., 1992
Proceedings of the Ocean Drilling Program, Scientific Results, Vol. 125

9. IGNEOUS STRATIGRAPHY AND MAJOR-ELEMENT GEOCHEMISTRY OF HOLES 786A AND 786B[1]

R. J. Arculus,[2] J. A. Pearce,[3,4] B. J. Murton,[4,5] and S. R. van der Laan[6,7]

ABSTRACT

A morphologically complex igneous basement was penetrated at Leg 125 Site 786 beneath approximately 100 m of Eocene-Pleistocene sediments at 31°52.45′N, 141°13.59′E in a 3082-m water depth. The site is located on the forearc basement high (FBH) of the Izu-Bonin (Ogasawara) Arc. In the broadest terms, the sequence in Hole 786B consists of a basal sheeted dike complex, heavily mineralized in places, with overlying pillow lavas giving way to a complex and repeated sequence of interlayered volcanic breccias and lava flows with some thin sedimentary intervals. The sequence has been further cut by dikes or sills, particularly of high-Ca and intermediate-Ca boninite, and is locally strongly sheared by faulting. The whole basement has been covered with middle Eocene-early Pleistocene sediments. A monomict breccia forms the shallowest portion of Hole 786B and a polymict breccia having Mn-oxide-rich clast coatings and matrix forms the deepest part of Hole 786A (~100–160 mbsf). The basement is tectonized in some places, and a mineralized stockwork is present in the deepest part of Hole 786B. A wide variety of rock types form this basement, ranging from mafic to silicic in character and including high-, intermediate-, and low-Ca boninites, intermediate- and low-Ca bronzite andesites, andesite, dacite, and rhyolite groups. Intragroup and intergroup relationships are complicated in detail, and several different upper mantle source(s) probably were involved. A significant role for orthopyroxene-clinopyroxene-plagioclase fractionation is indicated in the mafic-intermediate groups, and the most probable complementary cumulates should be noritic gabbros.

Many overall similarities but some subtle differences are noted between the igneous basement at Site 786 and the subaerial outcrops of the FBH to the south in the type boninite locality of Chichijima. Both suites were derived by hydrous melting of a relatively shallow, refractory (harzburgitic) upper mantle source. These Bonin forearc basement rocks are similar in many respects to those of Eocene-Oligocene age now forming the forearc of the Marianas at Leg 60 Site 458 and on Guam. In sharp distinction, the geochemistry of the Eocene-Pleistocene ash sequences overlying the Bonin FBH must have been derived from a very different upper mantle source, implying considerable across-strike differences in sub-arc mantle composition.

INTRODUCTION

The location of Leg 125 Holes 786A and 786B is at 31° 52.5′N, 141° 13.6′E, about 130 km east of Myojin Sho, the closest active subaerial volcano of the Izu-Bonin (Ogasawara) arc and about 70 km west of the axis of the Bonin Trench (Fig. 1). The drill site was chosen in about 3080-m water depth on a relatively thin sediment cover to achieve maximum basement penetration without reentry. A complex morphological variety of volcanic, hypabyssal, and sedimentary rock types is present at Site 786, represented by the following major units, as defined by the Shipboard Scientific Party (1990b) and abbreviated as follows:

Unit I (0–83.46 mbsf) consists of a succession of lower Pleistocene to middle Miocene nannofossil marls and clays.

Unit II (83.46–103.25 mbsf) is upper Oligocene to middle Eocene nannofossil marl and nannofossil-rich clays, including vitric ashes and mineral fragments.

Unit III (103.25–124.9 mbsf) is a sequence of middle Eocene volcaniclastic breccias.

Unit IV (124.9–166.5 mbsf in Hole 786A and 162.5–826.6 mbsf in Hole 786B) comprises massive and brecciated flows, ash flows, and intercalated vitric siltstones and sandstones in the upper part of the unit, and pillow lavas and dikes in the lower part.

The middle Eocene through early Pleistocene sedimentary Units I through III were recovered only from Hole 786A, whereas Unit IV represents the deepest part of the extended core-barrel (XCB)-drilled Hole 786A, and the total (661.1 m) cored using a rotary core bit (RCB) in Hole 786B. The final depth reached in Hole 786B was 828.6 mbsf, which represents a record for single-bit penetration into igneous basement.

This basement represents a continuation along strike of the "forearc basement high" (FBH) of Honza and Tamaki (1985), which shoals southward of Site 786 to a subaerial culmination in the Ogasawara Islands (including Chichijima) (Fig. 1).

The sedimentary cover of the FBH is cut by prominent canyons to the north (Aoga Shima Canyon) and south (Myojin Sho Canyon) of Site 786 (Klaus and Taylor, in press), but the basement is clearly continuous, with perhaps one right lateral offset at 30° N, southward to the Ogasawara Islands (Honza and Tamaki, 1985). Site 786 was, in fact, the contingency site for the FBH. The prime target was Site 782, located on the same FBH, about 120 km to the south of Site 786 (Fig. 1), but drilling barely penetrated basement beneath a relatively thick (~470 m) sediment cover. Despite the limited hard-rock recovery at Site 782, sufficient materials were obtained to permit documentation of considerable differences in the geochemical and petrological characteristics along the strike of the FBH between Sites 782 and 786. Variable petrochemistry of equivalent age has also been reported along strike in the Ogasawara Islands (Shiraki et al., 1980; Umino, 1985).

Here, we present the igneous stratigraphy and major-element geochemistry of Site 786. Some major-element comparisons are then made with suites from (1) other drilling legs in the forearcs of the Bonin-Mariana system, (2) lower Tertiary volcanic rocks exposed

[1] Fryer, P., Pearce, J. A., Stokking, L. B., et al., 1992. *Proc. ODP, Sci. Results,* 125: College Station, TX (Ocean Drilling Program).
[2] Department of Geology and Geophysics, University of New England, Armidale, N.S.W. 2351, Australia.
[3] Department of Geology, University of Newcastle-upon-Tyne, NE1 7RU, United Kingdom.
[4] Department of Geological Sciences, University of Durham, DH1 3LE, United Kingdom.
[5] Institute of Oceanographic Sciences, Godalming, Surrey, GU8 5UB, United Kingdom.
[6] California Institute of Technology, Division of Geological and Planetary Sciences 170-25, Pasadena, California 91125, U.S.A.
[7] School of Ocean and Earth Science and Technology, University of Hawaii, 2525 Correa Road, Honolulu, Hawaii 96822, U.S.A.

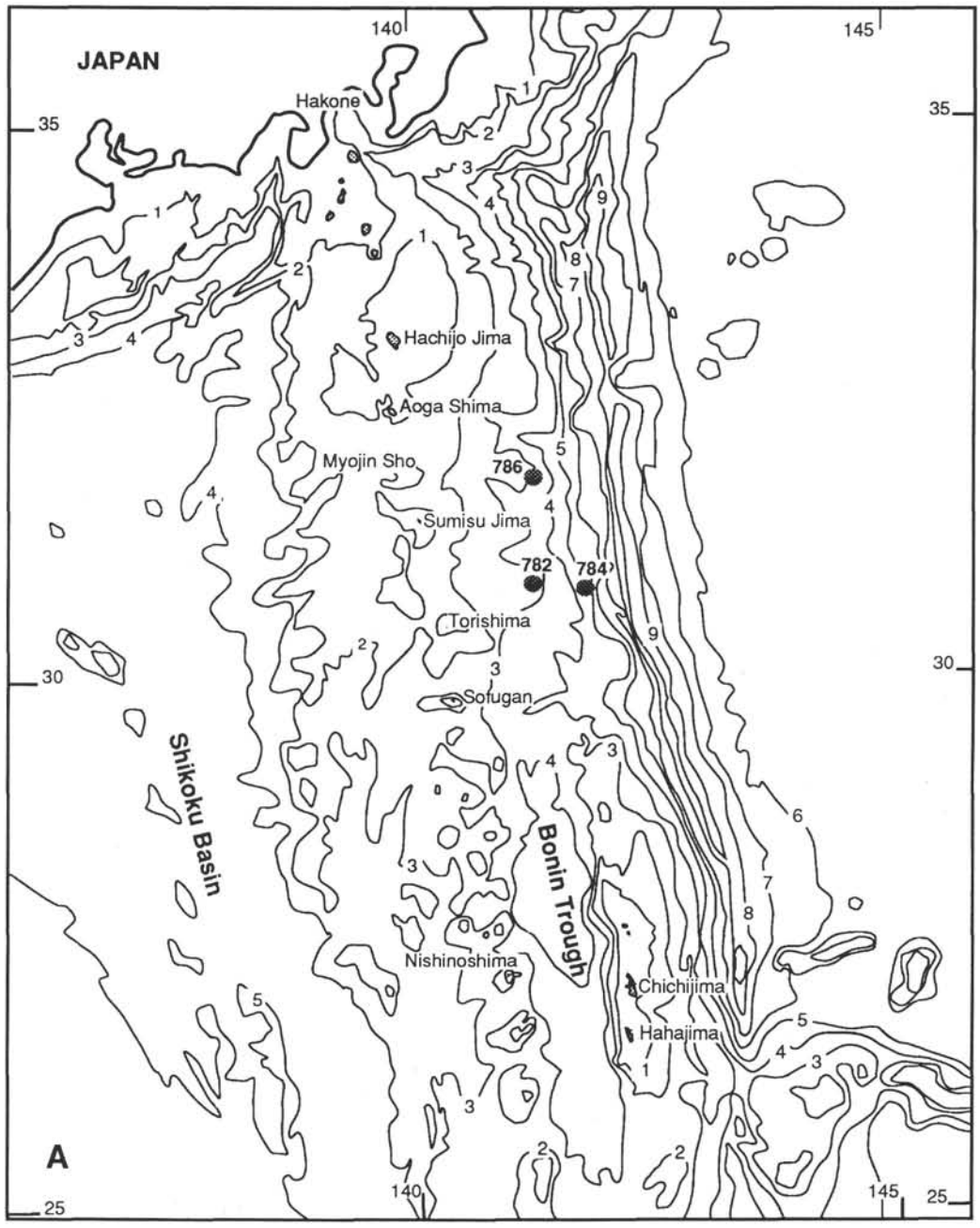

Figure 1. Location maps (general Izu-Bonin (**A**) and Site details (**B**)) for Leg 125 Site 786. Blathymetry and basement features are from Honza and Tamaki (1985) and Klaus and Taylor (in press). Depth contours are in kilometers.

subaerially on Chichijima and Guam, and (3) boninites from other locales. In addition, some general observations are offered with respect to the nature of the upper mantle sources involved in the construction of the Bonin forearc during the Tertiary and compared with those sources tapped by explosive arc activity during this same time period and preserved in ash layers of Holes 782A, 784A, and 786A (Arculus and Bloomfield, this volume).

IGNEOUS LITHOSTRATIGRAPHY

Hole 786A

Apart from a single analyzed igneous clast recovered in Sample 125-786A-6X-5, 24–27 cm, in nannofossil marls and clays of middle Miocene age, the majority of igneous rocks studied in this hole are clasts. These are in volcaniclastic breccias of middle Eocene age in Unit III (Section 125-786A-11X-5, 125 cm, to 125-786A-13X, CC, 44 cm) and the upper part of Unit IV (Section 125-786A-14X-1, 0 cm, to 125-786A-19X-1, 15 cm).

An increased clast content and dark-brown coloration marks the transition from the shallower units in Hole 786A. Clast colors are variable (white, yellowish brown through dark greenish-gray to black), and diameters are about 1 cm on average, with a minority up to 4 cm. In Unit IV, drilling abrasion has produced numerous chip- and pebble-sized igneous rock fragments. A general black coloration to the matrix sediment is caused by disseminated manganese oxide.

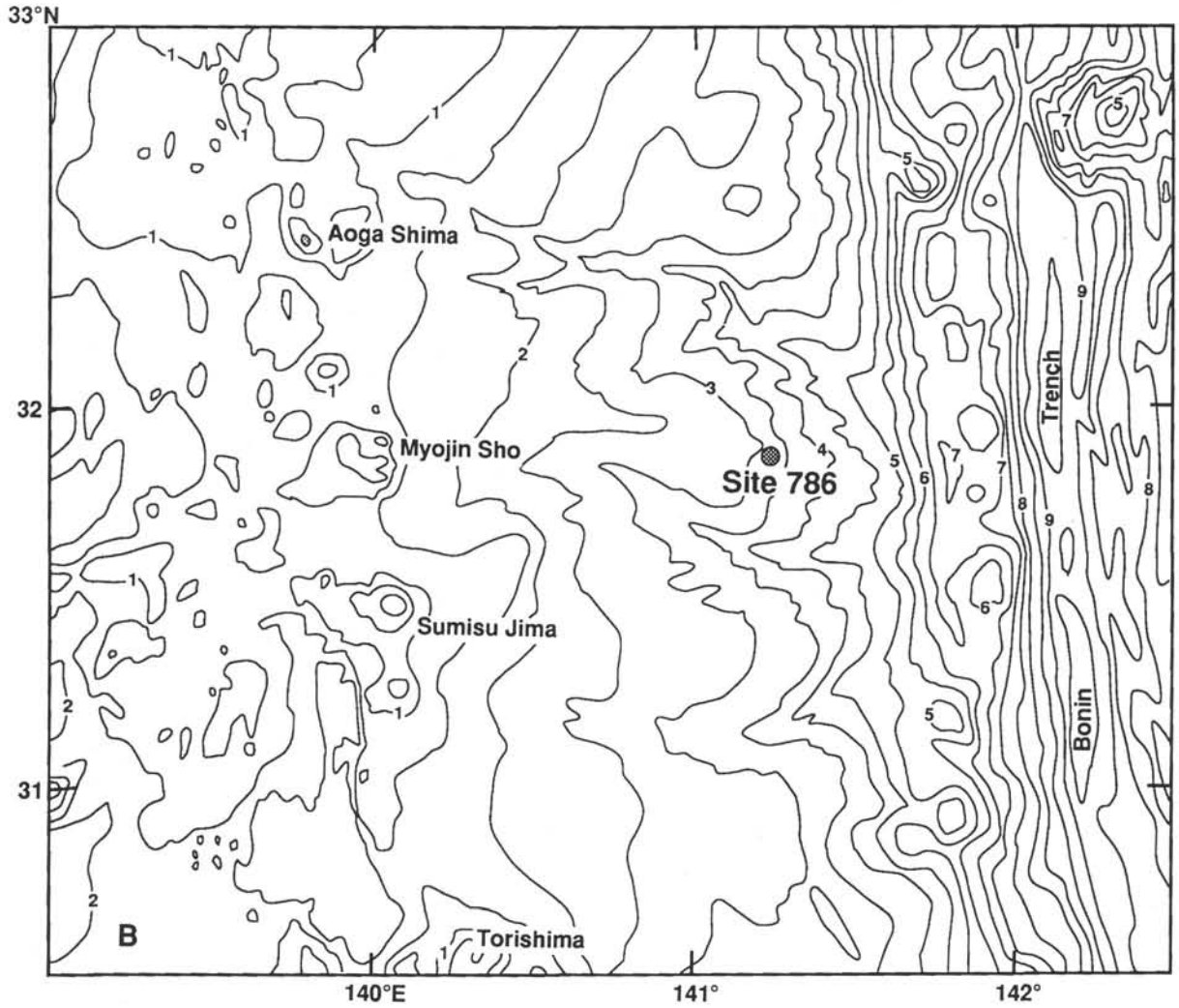

Figure 1 (continued).

Hole 786B

Lithologic Unit IV consists of dikes, sills, pillow lavas, lava, and pyroclastic flows, volcaniclastic breccias, conglomerates, vitric siltstones and sandstones, clayey siltstones, and sandstones. The biostratigraphic age determination for the top of this predominantly igneous basement is middle Eocene, and a number of sedimentary horizons intercalated with the igneous rocks deeper in Unit IV also yield fossil assemblages of this age. The K-Ar isochron of 41.3 ±0.5 Ma for the lavas and dikes of the volcanic edifice (excluding late-stage dikes and samples with obvious reset ages) is also consistent with this age (see Mitchell et al., this volume).

Here, Unit IV has been subdivided into 34 subunits on the basis of lithological contrasts (dikes and sills, breccias, flows, sedimentary and tectonized horizons) and geochemistry. We have identified eight major chemical groups, some of which occur in different lithologies (e.g., dike, flow, and breccia) at different horizons in the hole. A ninth chemical group represents a catch-all that lacks consistent characteristics, and to which the diverse clasts from the base of Hole 786A have been assigned.

With the available ages (Mitchell et al., this volume), we have some knowledge of the probable commonality of a number of dike/flow occurrences. However, not all of the subunits have been dated, and so we refrained from grouping the separate lithologies of the different chemical groups into single cooling units.

Some revisions, reassignments, and modifications of the subunits described by the Shipboard Scientific Party (1990b) have been recognized. A schematic lithostratigraphic section is displayed in Figure 2. Detailed core descriptions of the Shipboard Scientific Party (1990b) should be referred to for comprehensive morphological characterization (colors, vesicle dimensions, clast sizes, and alteration profiles). We emphasize, however, that many of the names employed at that time for the different rock types have been discarded, and alternatives have been introduced here. The chemical basis for these names and the full analytical data set description follows our presentation of the lithostratigraphy.

Two morphological problems caused particular difficulties for assignment of lithologies during core descriptions. The first of these is the distinction between dikes and flows. Chilled margins were rarely recovered during drilling and, in fact, overall recovery percentages were generally low (average, ~28.5%) in Hole 786B. Accordingly, a massive, avesicular character and rapidly alternating chemistry from one lithology to another are believed to be characteristic of dikes. The second problem concerns the recognition of brecciated dikes vs. brecciated pillow lavas, particularly in Cores 125-786B-45R-1—57R-1. A field trip to Chichijima under the guidance of S. Umino during 1990 was of immense help for R.J.A. and J.A.P. in resolving these descriptive difficulties. Many of the unequivocal dikes on Chichijima are prominently vesicular, and if volatile contents in the different magma types were broadly similar between Site 786 and Chichijima, an obvious

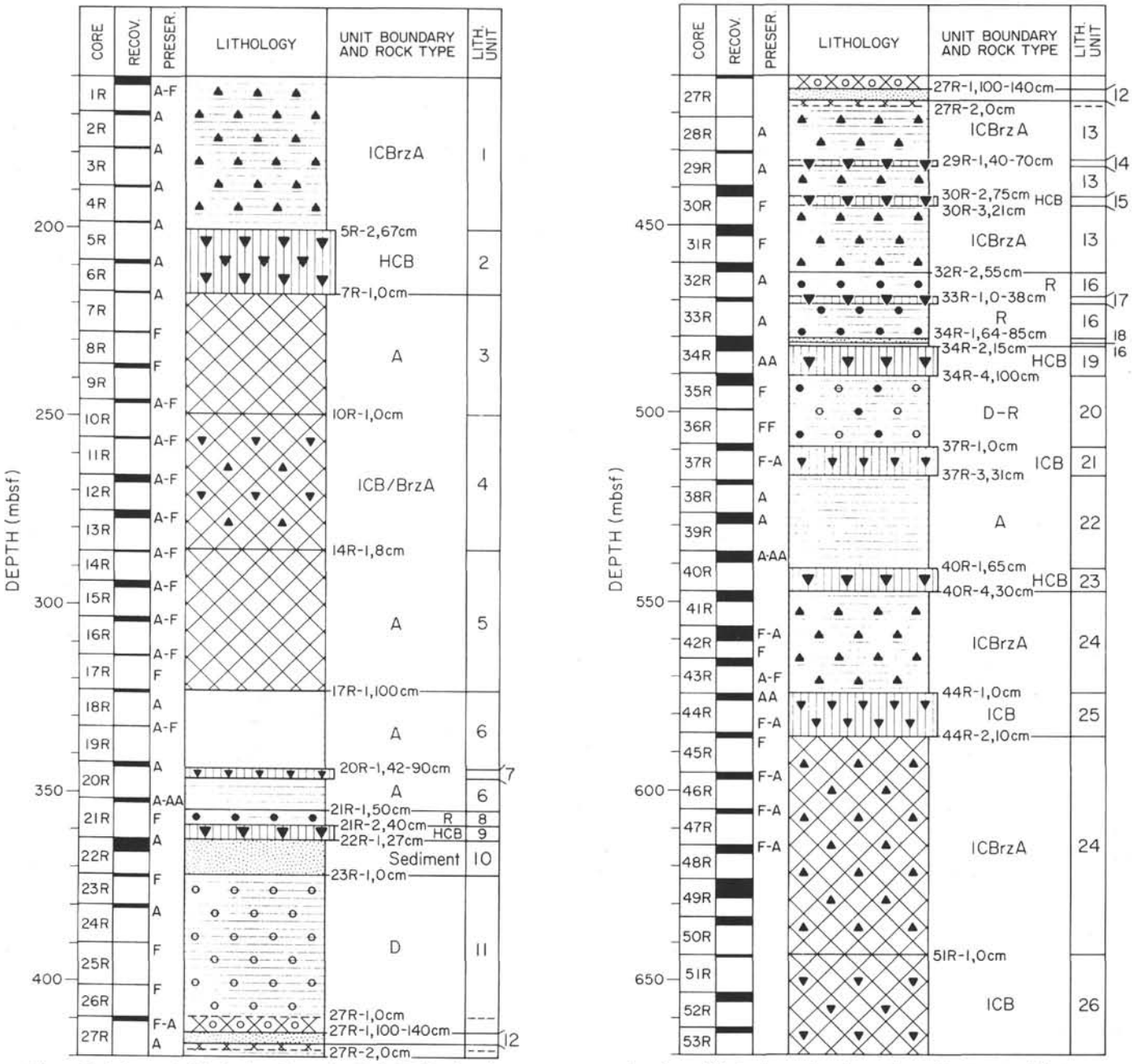

Figure 2. Schematic lithologic column for Hole 786B, showing core recovery fractions, lithologies and units, and notable structural features.

conclusion one can draw from the comparative field relations is that the level of intrusive exposure encountered at Site 786 must be deeper than that exposed on Chichijima. Note also that a remarkably consistent stratigraphy has been documented for this island over distances of some 10×3 km (Umino, 1985) and may indicate that the major lithologies encountered downhole can be extrapolated over distances of this scale.

Lithostratigraphy of Unit IV, Site 786

Unit IV has been subdivided into 34 subunits (IV-1 to IV-34) as shown in Figure 2. Breccias (polymict and monomict), lava flows including pillowed varieties, dikes, and sills are the most significant volumetrically, with relatively thin sedimentary horizons.

Subunit IV-1 (Sections 1256-786A-11X-5, 100 cm —19X, CC and Sections 125-786B-1R-1, 0 cm, —5R-2, 67 cm)

Polymict breccia (Sections 125-786A-11X-5, 100 cm, —19X, CC) and monomict flow breccias (Sections 125-786B-1R-1, 0 cm, —5R-2, 67 cm) with vesicular gray clasts of intermediate-Ca bronzite andesite supported by a light-green, hyaloclastite-rich matrix. In clasts near the base of this subunit (Sample 125-786B-5R-2, 30–45 cm), some magma mingling appears to be present, possibly due to partial fusion of the clasts by the underlying sill.

Subunit IV-2 (Sections 125-786B-5R-2, 67 cm—7R-1, 0 cm)

Dike or sill of high-Ca boninite, of variable color from dark gray to light, yellowish brown.

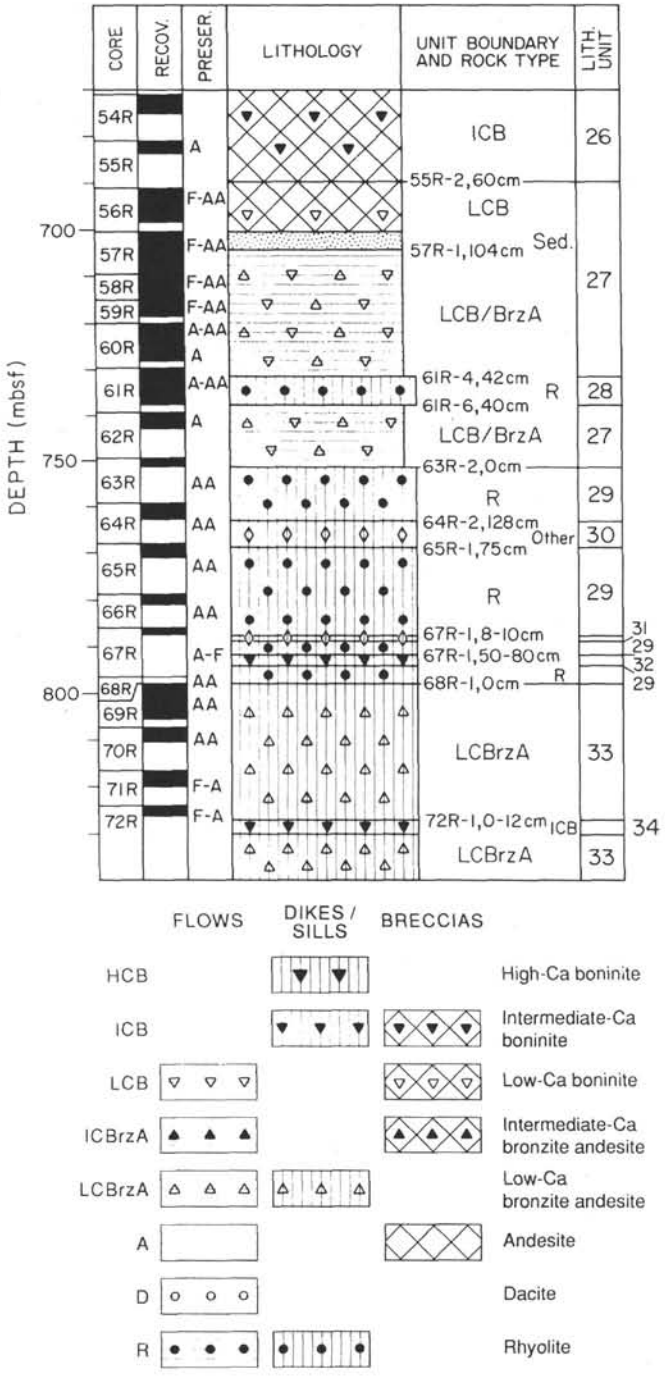

Figure 2 (continued).

Subunit IV-3 (Sections 125-786B-7R-1, 0 cm —10R-1, 0 cm)

Matrix-supported monomict breccia of andesite clasts, some with elongate and abundant vesicles, in a greenish gray to pale green matrix.

Subunit IV-4 (Sections 125-786B-10R-1, 0 cm—14R-1, 8 cm)

Matrix-supported polymict breccia of gray to greenish gray, intermediate-Ca boninite and bronzite andesite clasts, in a greenish gray matrix.

Subunit IV-5 (Sections 125-786B-14R-1, 8 cm—17R-1, 100 cm)

Matrix-supported polymict breccia of andesite and dacite clasts in a pale greenish gray matrix.

Subunit IV-6 (Sections 125-786B-17R-1, 100 cm—21R-1, 50 cm)

Vesicular andesite lava flow(s), strongly brecciated and sheared in Section 125-786B-21R-1, 0 cm—21R-1, 50 cm.

Subunit IV-7 (Section 125-786B-20R-1, 42–90 cm)

Sparsely vesicular intermediate-Ca boninite dike or sill (intruded into Subunit IV-6).

Subunit IV-8 (Sections 125-786B-21R-1, 50 cm—21R-2, 40 cm)

Flow-banded, oxidized, vesicular, glassy rhyolite lava or welded ash flow with a chill (vitrophyre) at the lower margin; uppermost contact is overlain by sandstone-siltstone having grains that apparently were derived from the underlying flow.

Subunit IV-9 (Sections 125-786B-21R-2, 40 cm—2R-1, 27 cm)

Dike or sill of high-Ca boninite.

Subunit IV-10 (Sections 125-786B-22R-1, 27 cm—23R-1, 0 cm)

Vitric sandstones and silts, together with fragmental rhyolitic materials; at the base this subunit is fine-grained and appears polymictic with fragments of tuff and contains many oxidized grains, overlain by bedded tuff (Sample 125-786B-22R-3, 78–82 cm) with flattened pumice fragments in Sample 125-786B-22R-3, 103–106 cm. A prominent 14-cm-thick layer of pink to grayish pink sepiolite, possibly of hydrothermal origin, occurs at the top of this subunit.

Subunit IV-11 (Sections 125-786B-23R-1, 0 cm—27R-1, 100 cm)

Vesicular dacite lava flows.

Subunit IV-12 (Sections 125-786B-27R-1, 100 cm—27R-2, 0 cm)

Greenish yellow, coarse- to fine-grained, bedded volcanic sandstone having altered lithic and vitric fragments, pyroxene crystals, and abundant hematite staining; cross-bedding and lamination developed at the base of the subunit.

Subunit IV-13 (Sections 125-786B-27R-2, 0 cm—32R-2, 55 cm)

Sparsely vesicular lava flows of intermediate-Ca bronzite andesite; Sample 125-786B-31R-2, 10–20 cm is a monogenic breccia with oxidized fragments.

Subunit IV-14 (Section 125-786B-29R-1, 40–70 cm)

Sparsely vesicular dike or sill of high-Ca boninite, intruded into Subunit IV-13.

Subunit IV-15 (Sections 125-786B-30R-2, 75 cm—30R-3, 21 cm)

Sparsely vesicular dike or sill of high-Ca boninite, intruded into Subunit IV-13; brecciated in Section 125-786B-30R-2, 75–105 cm.

Subunit IV-16 (Sections 125-786B-32R-2, 55 cm—34R-2, 15 cm)

Variably oxidized and altered, brecciated and flow-banded rhyolite flows, partly mineralized in Sections 125-786B-33R-1, 65 cm—34R-1,

64 cm. Fine-grained glassy tuffs, possibly welded in Sample 125-786B-34R-1, 113–117 cm, are present at the base of the Subunit.

Subunit IV-17 (Section 125-786B-33R-1, 0–38 cm)

Avesicular, oxidized dike or sill, probably of high-Ca boninite composition, intruded into Subunit IV-16.

Subunit IV-18 (Sections 125-786B-34R-1, 64 cm—34R-1, 85 cm)

Vitric sandstone and siltstone with some graded bedding and considerable oxidation of grains and matrix.

Subunit IV-19 (Sections 125-786B-34R2, 15 cm—786B-34R-4, 100 cm)

Massive dike of high-Ca boninite.

Subunit IV-20 (Sections 125-786B-34R-4, 100 cm—37R-1, 0 cm)

Vesicular lava flows of dacite-rhyolite.

Subunit IV-21 (Sections 125-786B-37R-1, 0 cm—37R-3, 31 cm)

Moderately oxidized, intermediate-Ca boninite dike or sill.

Subunit IV-22 (Sections 125-786B-37R-3, 31 cm—40R-1, 65 cm)

Vesicular andesite lava flows and breccia, having crystalline and palagonitized fragments, and considerable hematitic alteration on clast rims and in the matrix.

Subunit IV-23 (Sections 125-786B-40R-1, 65 cm—40R-4, 30 cm)

High-Ca boninite dike or sill.

Subunit IV-24 (Sections 125-786B-40R-4, 30 cm—51R-1, 0 cm)

Breccia and vitric sandstones, having many angular and some hematized fragments in Sections 125-786B 40R-4, 30 cm—42R-2, 50 cm, overlying lava flows and possible dikes of intermediate-Ca bronzite andesite. Matrix-supported breccia with angular fragments of intermediate-Ca bronzite andesite comprises Sections 125-786B-44R-2, 10 cm —51R-1, 0 cm. The matrix in Sections 125-786B-48R-2 and -49R-2 is pervasively oxidized.

Subunit IV-25 (Sections 125-786B-44R-1, 0 cm—44R-2, 10 cm)

Dike or sill of intermediate-Ca boninite, intruded into Subunit IV-24.

Subunit IV-26 (Sections 125-786B-51R-1, 0 cm—55R-2, 60 cm)

Matrix-supported, polymict volcanic breccia having clasts of intermediate-Ca boninite and bronzite andesite in Sections 125-786B-51R-1, 0 cm—55R-2 inclusive; larger clasts are dark, other are gray to dark gray. Matrix is dark green to greenish gray.

Subunit IV-27 (Sections 125-786B-55R-2, 60 cm—63R-2, 0 cm)

Pillow lavas and hyaloclastite (glass-rich sandstones and breccias) of low-Ca boninite and bronzite andesite with pillow dimensions on the order of 1 m wide; contorted and coliform hematite-rich sediments between some pillows, white and green zeolites, and hematite filling some veins and vesicles. Vitric sandstone with basal graded bedding, locally clast-bearing and fining upward, in Section 125-786B-57R-1, 0 cm—57R-1, 104 cm. A fault breccia forms the basal contact with Subunit IV-29.

Subunit IV-28 (Sections 125-786B-61R-4, 42 cm—61R-6, 40 cm)

Locally oxidized rhyolite dike, intruded into and brecciated near the contacts with subunit IV-27.

Subunit IV-29 (Sections 125-786B-63R-2, 0 cm—68R-1, 0 cm)

Variably chloritized and albitized rhyolite dikes, locally sulfide-bearing with zeolite, carbonate and chlorite filling vesicles.

Subunit IV-30 (Sections 125-786B-64R-2, 128 cm—65R-1, 75 cm)

Massive andesite dike or sill, intruded into Subunit IV-29.

Subunit IV-31 (Sections 125-786B-67R-1, 8 cm—67R-1, 10 cm)

Dike stringer of intermediate-Ca boninite, intruded into Subunit IV-29.

Subunit IV-32 (Sections 125-786B-67R-1, 50 cm—67R-1, 80 cm)

Intermediate-Ca boninite dike, extensively chloritized with local vein fillings of carbonate and sulfide, intruded into Subunit IV-29.

Subunit IV-33 (Sections 125-786B-68R-1, 0 cm—72R-2, 150 cm)

Dikes of low-Ca bronzite andesite; evidence of extensive chloritization, mineralization with sulfides, and presence of carbonate along fractures. Argillized and mineralized stockwork in Sections 125-786B-71R-1, 0 cm –125-786B-71R-4, 0 cm; igneous host has been extensively altered to clay minerals, epidote, chlorite, and quartz.

Subunit IV-34 (Sections 125-786B-72R-1, 0 cm—72R-1, 12 cm)

Dike of chloritized intermediate-Ca bronzite andesite, intruded into Subunit IV-33.

In the broadest terms, the sequence in Hole 786B consists of a basal sheeted dike complex, heavily mineralized in places, with overlying pillow lavas giving way to a complex and repeated sequence of interlayered volcanic breccias and lava flows with some thin sedimentary intervals. The sequence has been further cut by dikes or sills, particularly of high-Ca and intermediate-Ca boninite, and is locally strongly sheared by faulting. The whole basement has been covered with middle Eocene-early Pleistocene sediments. In part, therefore, this sequence is analogous to the upper portions of some ophiolites, especially those that have been called "supra-subduction zone" types by Pearce et al. (1984).

It seems likely that many of the components of the polymict breccias were derived from local sources in view of: (1) large clast dimensions (<20 cm), (2) angular shapes of many of the clasts, and (3) similarity of composition between clasts and lavas or pillows and dikes. The predominant local source may well have been a prominent volcanic edifice.

The matrix-supported character of the breccias is consistent with mass-flow deposition with localized high relief. Similarly, the structures present in vitric sandstones and siltstones (normal size-grading, syndepositional slump structures, and cross-bedding) are indicative of mass-flow and resorting processes.

On the basis of surficial oxidation characteristics of the clasts and the apparent development of pyroclastic flows at shallower levels in Hole 786B, we believe that there was a shoaling of the local region to subaerial conditions (Lagabrielle et al., this volume). Oxidized clasts are also present in the uppermost, volcanic-derived formation (Mikazukiyama) on Chichijima, and similar subaerial sources have

been inferred, although no evidence exists for the emergence of Chichijima itself (Umino, 1985). During field studies of Hahajima, however, mappers have identified a within-unit transition from subaerial pyroclast flow to submarine debris flow deposition conditions (S. Umino, pers. comm., 1990), and thus evidence does exist for near sea level to subaerial activity during the middle Eocene construction of the present-day FBH.

The fossil fauna present in sediments immediately overlying the basement at Site 786 lived at a >1000 m depth (Milner, this volume). It is possible, therefore, that if Site 786 emerged above sea level for any period of time, rapid subsidence followed. This is unlike the case farther south on the FBH, where upper Oligocene-Miocene shallow water limestones cap the volcanic formations on Chichijima and its vicinity.

ANALYTICAL TECHNIQUES

Shipboard

Representative lithologies were finely ground in a tungsten carbide (WC) barrel (~47 samples) from Holes 786A and 786B were analyzed on board the *JOIDES Resolution* using an automated ARL8420 (3 kW) X-ray fluorescence (XRF) spectrometer, equipped with a Rh target, for both major and trace elements. Fused disks of dried, oxidized sample powder, plus a lithium borate flux (with La_2O_3 as a heavy absorber) in a 1:12 dilution were prepared for major-element analysis.

Melting at 1150° C, homogenization for 10 min. and casting were performed using a Claisse Fluxer. The 1:12 dilution is designed to render intersample and sample-standard matrix effects insignificant, and linear calibrations based on a set of United States, Japan Geological Survey, and Centre de Recherches Petrographiques et Géochemiques international standards, were used.

Five-g pressed powder pellets with a polyvinyl alcohol (PVA) binder were used to determine trace elements. Matrix absorption corrections were made through a modified Compton back-scattering technique. For the suite of trace elements determined for Site 786, the most energetic wavelength analyzed (Nb K_a) required a minimum of 4.5 g of powder for effective infinite thickness.

Shore-based

An additional set of 102 samples was selected from Hole 786B (1) to provide extra lithological coverage, particularly near the bottom of the hole where time constraints on board the ship had restricted the number of analyzed samples, and (2) to check the accuracy of the on-board analyses.

Portions of this sample set were distributed between the Universities of Durham, Hawaii, and New England (UNE) for (1) trace-element analysis by inductively-coupled, plasma source spectroscopy; (2) dating by the K-Ar method; (3) radiogenic isotope (Sr-Nd-Pb) analysis by solid-source mass spectrometry; (4) mineral analyses by electron microprobe; and (5) major- and trace-element analysis by X-ray fluorescence (XRF). Results of studies (1) through (4) are presented in Murton et al., Mitchell et al., Pearce et al., and van der Laan et al., respectively (this volume).

In the case of the bulk major- and trace-element XRF analyses at UNE, the samples were finely ground in a WC mill, and fused disks were prepared with a lithium tetraborate flux (containing La_2O_3 as a heavy absorber) and ammonium nitrate as an oxidizer (and S as SO_4 retainer) in a dilution ratio of 1:5.4. Disks were made in a semi-automated, self-agitated furnace at 1050°–1100° C. An automated Siemens SRS300 (3 kW) spectrometer equipped with an end-window Rh target X-ray tube was employed. A modified version of the iterative matrix correction procedure of Norrish and Hutton (1969) was used, with a set of international standards as primary calibrants.

Trace-element analyses were completed for pressed powder pellets (5–10 g of sample where available) with a PVA binder. Matrix absorption corrections were made on the basis of analyzed major-element compositions and calibrations based on international standards and spiked synthetics.

RESULTS

Shipboard-UNE Comparisons

For seven samples from Site 786, a direct interlaboratory comparison of some of the analytical results is possible (Table 1). In the case of some of these samples, an inadequate volume of material remained after distribution for other analytical techniques for trace-element analysis at UNE.

For the majority of elements, the analytical agreement is excellent. In the case of two, however, significant differences among laboratories are evident. Most striking is the case of Na and less obvious is that of Ti. An overall graphical comparison of the Na and Ti results is presented in Figure 3. A bimodal distribution is apparent for Na, with the abundances determined on board the ship being lower by about 50%.

We are convinced in this case that the shipboard results are in error, because cross-checks with the XRF laboratory at the University of Michigan confirm the values obtained at UNE. A possible explanation of the shipboard results is that excessive evaporative loss of Na during disk preparation occurred, perhaps from higher temperatures of fusion for the Site 786 samples than those used to manufacture the standard disks.

Although the discrepancy between shipboard and UNE Ti results is not so obvious (Fig. 3), it appears that the abundances determined on board the ship are again too low. Evaporative loss during disk manufacture is an unlikely explanation in the case of Ti, but at low concentration levels, as is the case for the great majority of samples from Site 786, it is possible either that counting times and resulting precision were inadequate (especially given the high flux:rock mass used and the inherent, relatively poor fluorescence of the Ti X-ray by Rh-target tubes) or that a calibration problem exists.

In an attempt to rectify some of these problems, the original shipboard pressed powder pellets were run through the "majors-on-powders" system at the University of Durham, using an automated Philips PW 1400 XRF spectrometer with an iterative mass absorption correction and a closely related set of rock standards. The Na and Ti values thus obtained are higher than those determined on board the *JOIDES Resolution* and are similar to those determined at UNE.

The major- and trace-element data sets, from the UNE laboratory, the JOIDES *Resolution* (with modification of the on-board Na and Ti results with values obtained at the University of Durham), and a combined data set with major elements presented normalized to 100% volatile-free, are presented in Tables 2, 3, and 4, respectively.

The volatile contents of the majority of these samples clearly are not easily related to pristine magmatic values. Intersample and intersuite comparisons are not confused by variable volatile contents if whole-rock compositions are projected while excluding volatiles.

MgO-SiO_2 relationships and CaO contents have been established by Crawford et al. (1989) as important variables in the subdivision of boninite series volcanic rocks. MgO-SiO_2 and CaO-SiO_2 plots are therefore used in conjunction with the stratigraphic relationships and the mineralogical criteria of van der Laan et al. (this volume), as the basis for classification of the igneous samples from Site 786. These plots are shown in Figure 4.

We found eight distinct groups (indicated on Fig. 4) could be identified, namely: low-Ca boninite (LCB), intermediate-Ca boninite (ICB), high-Ca boninite (HCB), intermediate-Ca bronzite andesite (ICBrzA), low-Ca bronzite andesite (LCBrzA), andesite (A), dacite (D), and rhyolite (R). A few samples, particularly from Hole 786A, were assigned to a separate Group 9 that is a catch-all for compositions that are predominantly mafic in character, possibly heavily altered, but clearly heterogeneous. An obvious analytical target for further detailed study is the polymict breccia recovered from the bottom of Hole 786A, which is the source of most of these samples. The term rhyolite is used for rocks with >70 wt% SiO_2. Equivalent composi-

Table 1. Comparative major- and trace-element data for duplicate samples analyzed on board and at the University of New England (une). Other abbreviations are as follows: odp, Ocean Drilling Program; lab, laboratory where analysis was completed. All Fe reported as Fe_2O_3.

Sample 125-786A-	lab	SiO_2	TiO_2	Al_2O_3	Fe_2O_3	MnO	MgO	CaO	Na_2O	K_2O	P_2O_5	S	LOI
8-1, 43–44 cm	une	56.82	0.29	18.46	7.76	0.12	4.34	7.95	3.59	0.63	0.03	0.01	5.01
8-1, 45–47 cm	odp	56.76	0.23	18.25	8.10	0.13	4.16	8.03	2.37	0.68	0.05	0.00	2.71
9-1, 10–15 cm	odp	59.09	0.24	17.98	7.83	0.12	4.03	7.92	2.07	0.60	0.00	0.00	1.97
9-1, 15–17 cm	une	56.43	0.30	18.53	7.93	0.12	4.61	8.17	3.38	0.48	0.03	0.01	4.56
12-2, 120–124 cm	odp	61.39	0.12	13.24	7.37	0.12	8.68	6.96	1.56	0.46	0.03	0.00	1.53
12-2, 124–126 cm	une	59.28	0.19	13.72	7.75	0.13	8.82	7.08	2.56	0.44	0.02	0.01	3.17
16-1, 135–138 cm	une	64.68	0.30	15.76	6.78	0.10	2.03	5.77	3.86	0.69	0.04	0.00	3.43
16-1, 137–141 cm	odp	64.94	0.25	15.68	7.08	0.09	1.69	5.77	2.86	0.76	0.04	0.00	2.48
21-1, 26–29 cm	odp	59.86	0.27	17.85	8.11	0.11	1.95	6.91	2.80	0.90	0.15	0.00	2.91
21-1, 26–30 cm	une	60.57	0.32	17.75	7.27	0.07	1.75	6.71	4.33	0.87	0.33	0.02	5.21
51-1, 49–56 cm	une	56.12	0.21	13.17	8.41	0.16	11.20	7.81	2.38	0.36	0.16	0.03	3.91
51-1, 51–55 cm	odp	54.24	0.15	12.98	8.65	0.17	12.59	7.92	1.17	0.26	0.25	0.00	2.01
		Nb	Zr	Y	Sr	Rb	Zn	Cu	Ni	Cr	Ce	Ba	V
8-1, 43–44 cm	une												
8-1, 45–47 cm	odp	0.9	50.6	16.1	227.2	8.5	72.6	68.0	41.4	7.6	7.6	17.2	235.6
9-1, 10–15 cm	odp	1.6	52.9	10.4	225.6	6.6	71.5	101.0	39.8	8.1	15.7	40.0	238.6
9-1, 15–17 cm	une												
12-2, 120–124 cm	odp	2.1	37.0	6.5	166.1	6.3	53.4	73.6	115.7	424.7	12.5	37.2	186.9
12-2, 124–126 cm	une	0.0	35.0	6.0	157.0	6.0	65.0	58.0	127.0	564.0	0.0	42.0	184.0
16-1, 135–138 cm	une												
16-1, 137–141 cm	odp	1.5	57.4	10.0	216.9	7.2	64.6	90.9	8.8	5.8	15.4	35.3	218.5
21-1, 26–29 cm	odp	0.9	58.0	20.7	236.1	11.1	86.3	61.6	18.2	4.7	12.2	27.4	214.0
21-1, 26–30 cm	une	0.0	56.0	28.0	233.0	13.0	59.0	78.0	16.0	17.0	19.0	54.0	190.0
51-1, 49–56 cm	une	1.0	33.0	17.0	151.0	5.0	67.0	44.0	196.0	921.0	14.0	56.0	212.0
51-1, 51–55 cm	odp	0.5	37.1	17.4	166.3	3.7	70.3	40.9	195.0	659.1	20.0	22.4	227.5

tions also occur on Chichijima but are classified as quartz dacite by Umino (1986) on the basis of the absence of alkali feldspar phenocrysts.

Group names, prominent chemical characteristics, and a summary of lithological occurrences are presented in Table 5.

A prime observation that one can make about the CaO-SiO_2 and MgO-SiO_2 plots in Figure 4 is that a spectacular range of compositions is present that extends over all of the so-called boninite types of Crawford et al. (1989) (see also Fig. 6). The end-members of the range recovered from Hole 786B are very MgO-rich SiO_2-poor and high-SiO_2 rocks respectively. Some other generally important chemical characteristics are as follows:

1. Many of the samples are characterized by relatively high MgO contents at intermediate SiO_2 contents (Fig. 4).
2. As a consequence of high MgO contents and low FeO*/MgO ratios (where FeO* is total Fe expressed as FeO), most of this suite of rocks projects within the calc-alkalic field of Miyashiro's (1974) discriminant plot (Fig. 5).
3. Except for Sample 125-786A-6X-5, 24–27 cm, all samples have strikingly low TiO_2 abundances compared with those of active, subaerial arc systems (Fig. 7) or mid-ocean ridge basalts (N-MORB has, for example, on average about 1.5 wt% TiO_2).

Note that, although a broad spectrum of degrees of alteration of original magmatic mineralogy and glass content exists at Site 786 (up to greenschist facies albite-chlorite-epidote-quartz assemblages), the major oxides used for classification appear relatively robust with respect to this alteration. A measure of this robustness is the survival of the group assignments on the basis of mineralogical characteristics, immobile trace-element abundances, and distinctive isotopic ratios. However, it appears that the low-Ca bronzite andesites (Group 5) have experienced significant K-loss (see below), but this group is distinctive on the basis of less mobile major and trace elements. Abnormally high P_2O_5 contents are present in a number of andesite (Group 6) samples (see Table 4), probably the result of P mobility in fluids circulating within the volcanic pile.

When assigning group names, we attempted to conform with the current usage of terms like boninite and bronzite andesite, as documented by students of the Guam, Leg 60, and Chichijima suites (e.g., Reagan and Meijer, 1984; Hickey-Vargas, 1989; Umino, 1985, 1986). At this point, however, we stress that some difficulty was encountered with the current usage of "boninite" (Peterson, 1891), given that this term is actually applied as a petrographic distinction (olivine-orthopyroxene ± clinoenstatite-spinel in a glassy matrix) within a compositional class that might otherwise be called "high-Mg andesite" (see various chapters in Crawford (1989) for further discussion).

A compositional gap exists between the boninite and bronzite andesite groups of Site 786 in a plot of wt% MgO vs. SiO_2 (Fig. 4). Analyses of type boninites from Chichijima (Umino, 1986) project within this gap (Fig. 6). Accordingly, some of the Site 786 samples labeled boninite here might be regarded as too SiO_2-poor to merit the terms boninite or high-Mg andesite. This is particularly significant with respect to the high-Ca boninites (Group 1), which when dated, have all proved younger than most other boninite and bronzite andesite groups of Site 786, giving Oligocene and Miocene ages— see Mitchell et al., (this volume). Nevertheless, this high-Ca boninite group is similar in many respects to other high-Ca boninites (Crawford et al., 1989) from other localities, such as the Troodos Ophiolite (Fig. 6). Similarly, the rocks identified here as low-Ca bronzite andesites (Group 5) are similar to Tertiary boninites from New Caledonia (Cameron, 1989) (Fig. 6), but given the relatively low MgO and high SiO_2 content of Group 4, we prefer the term bronzite andesite.

By way of comparison of the compositional spread from Site 786 to a representative subaerial arc suite of basalt-andesite-dacite-rhyolite, compositions from Hakone (Honshu, Japan, Fig. 1) are shown in Figure 7. First, the distinctly higher MgO content at a specific SiO_2 content of the Site 786 rocks, compared with the Hakone suite (which includes both tholeiitic and calc-alkalic types on the basis of Miyashiro's (1971) discriminant), is distinctive. Second, the low-Ca types (boninite Group 3 and bronzite andesite Group 5) from Site 786 are distinctly poorer in CaO than are volcanic rocks from Hakone at equivalent SiO_2 contents. Finally, some similarity exists in terms of CaO-MgO-SiO_2 characteristics between the intermediate-to-silicic

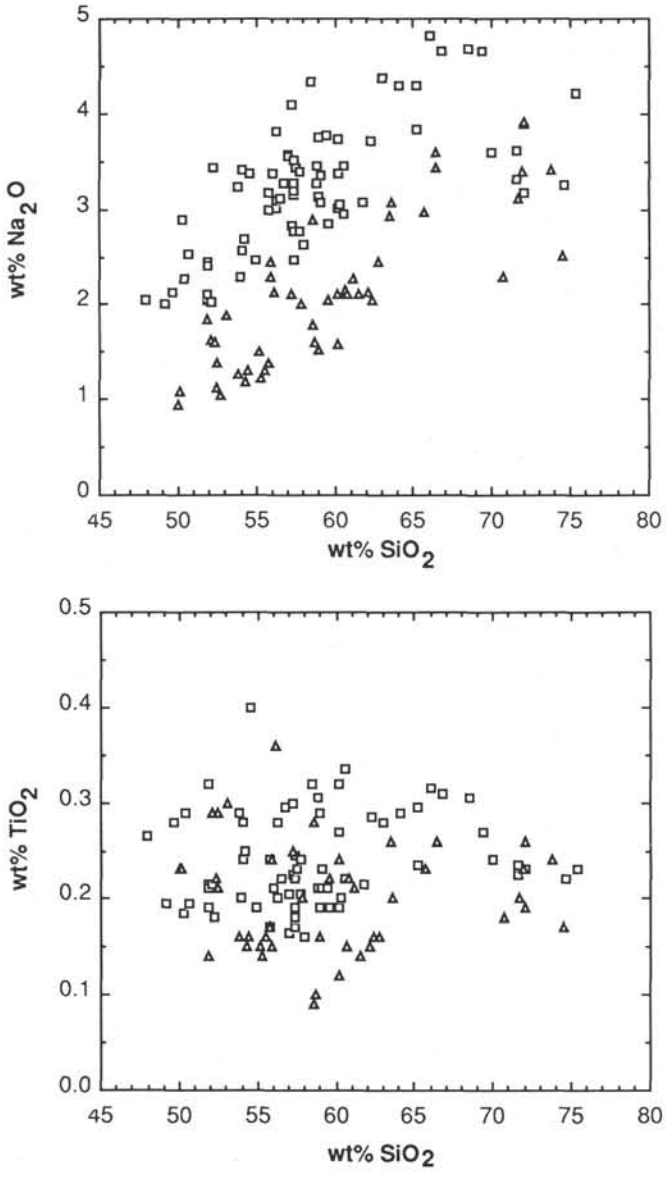

Figure 3. Variation of wt% Na_2O and TiO_2 with respect to SiO_2 for the sample suites analyzed on board the *JOIDES Resolution* (triangles) and at the University of New England (squares).

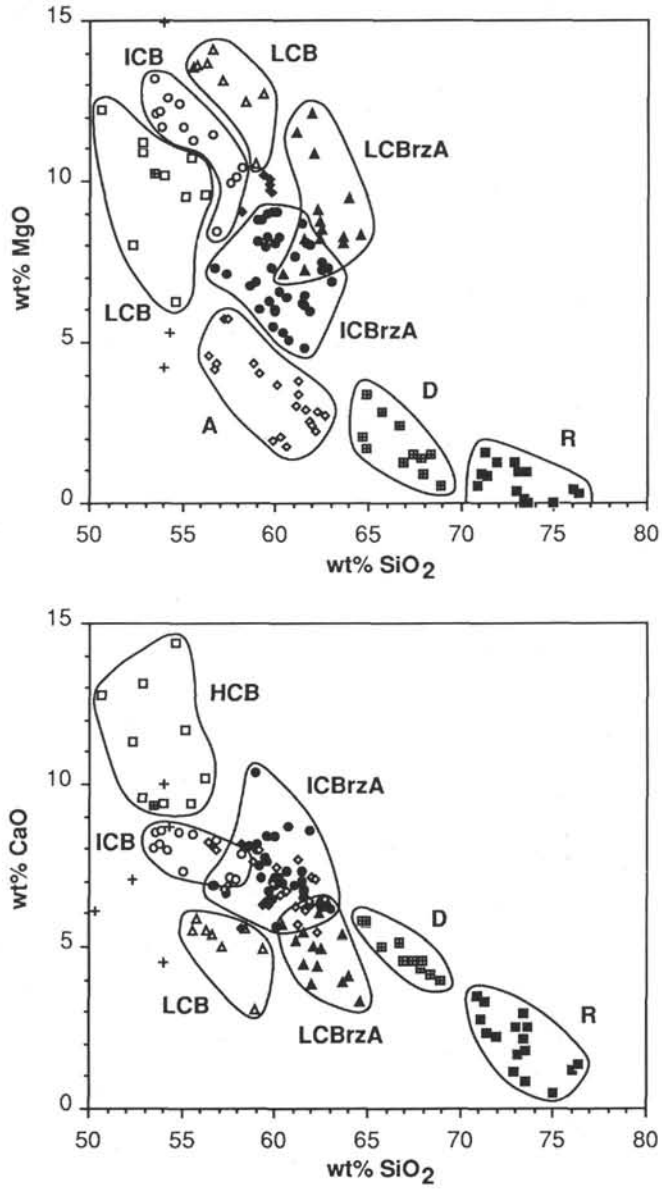

Figure 4. Wt% MgO and wt% CaO vs. wt% SiO_2 for all analyzed rocks from Holes 786A and 786B. The abbreviations attached to the group fields are as follows: HCB, High-Ca boninite; ICB, intermediate-Ca boninite; LCB, low-Ca boninite; ICBrzA, intermediate-Ca bronzite andesite; LCBrzA, low-Ca bronzite andesite; A, andesite; D, dacite; R, rhyolite. The crosses are the Group 9 (undifferentiated) samples. The samples (Group 2-4) intermediate between the intermediate-Ca boninite and intermediate-Ca bronzite andesite are indicated by filled diamonds.

members of the Hakone suite and the andesite, dacite, and rhyolite groups of Site 786.

Accordingly, the names andesite-dacite-rhyolite, as applied to specific Groups 6, 7, and 8 from Site 786, seem appropriate in view of some of their major-element characteristics, but distinctive minor- and trace-element differences also exist between these groups at Site 786 and active, subaerial arc systems.

Petrogenetic Relations Between Groups

There is an overall coherence of some aspects of the geochemistry of the basement at Site 786 (e.g., low TiO_2, Pb isotopic characteristics see Pearce et al., this volume), implying the persistent involvement of the same source(s) in the genesis of the magmas. However, there are also significant differences in critical trace-element ratios (Murton et al., this volume) and Sr-Nd isotopic values (Pearce et al., this volume) that indicate in detail that more complex petrogenetic processes were important.

Within and between some groups, the sources of chemical variability may be accounted for by combinations of fractional crystallization (including crystal accumulation or flotation) and magma mixing (see also Umino, 1986).

Particularly useful graphical tools for exploring these relationships are Pearce-type plots (e.g., Pearce, 1968). Given the relatively simple igneous mineralogy of the Site 786 suite (olivine-Cr-spinel-orthopyroxene-clinopyroxene-plagioclase-quartz; van der Laan et al., this volume), it is possible to test in a straightforward way for the

Table 2. Major- and trace-element analyses, obtained at the University of New England, of representative lithologies from Site 786.

Sample	Depth (mbsf)	SiO_2	TiO_2	Al_2O_3	Fe_2O_3*	MnO	MgO	CaO	Na_2O	K_2O	P_2O_5	S	LOI	Total
125-786B-														
1R-1, 25–28 cm	162.75	57.21	0.23	13.03	6.95	0.12	7.70	6.52	2.83	0.58	0.16	0.01	4.01	99.34
1R-1, 75–79 cm	163.25	57.32	0.19	11.92	6.80	0.11	7.51	5.74	2.77	0.61	0.03	0.01	2.81	95.81
1R-1, 89–93 cm	163.39	60.28	0.20	12.53	6.72	0.11	7.00	6.00	3.06	0.51	0.03	0.04	3.35	99.82
2R-1, 72–76 cm	170.22	60.12	0.19	12.40	6.76	0.11	7.00	5.98	3.01	0.48	0.03	0.01	3.11	99.18
3R-1, 34–44 cm	170.35	60.55	0.22	12.49	6.87	0.11	7.26	6.03	2.96	0.47	0.03	0.00	2.95	99.92
4R-1, 109–111 cm	179.54	61.77	0.22	12.86	6.72	0.11	6.72	6.02	3.07	0.56	0.03	0.00	1.93	99.99
5R-1, 23–25 cm	190.09	57.35	0.25	14.70	6.78	0.10	5.69	6.78	3.19	0.74	0.02	0.01	4.40	100.00
5R-2, 1–6 cm	200.33	59.12	0.23	14.33	6.50	0.11	5.89	6.27	3.08	0.47	0.03	0.01	3.68	99.70
6R-3, 17–22 cm	211.37	51.88	0.32	14.25	8.25	0.16	9.81	9.05	2.10	0.21	0.04	0.00	3.84	99.90
8R-1, 43–44 cm	228.03	54.00	0.28	17.55	7.38	0.11	4.12	7.55	3.42	0.60	0.03	0.01	5.01	100.05
9R-1, 15–17 cm	237.25	53.83	0.29	17.68	7.57	0.12	4.40	7.79	3.23	0.46	0.03	0.01	4.56	99.94
11R-1, 103–108 cm	257.33	54.86	0.19	13.46	7.57	0.13	9.47	6.76	2.46	0.37	0.01	0.01	4.72	99.99
12R-2, 124–126 cm	266.67	57.40	0.18	13.29	7.50	0.13	8.54	6.86	2.48	0.43	0.02	0.01	3.17	99.98
13R-2, 134–138 cm	278.47	59.55	0.19	13.50	6.71	0.11	7.44	6.67	2.86	0.50	0.03	0.00	2.37	99.93
15R-2, 3–8 cm	296.53	56.78	0.30	15.90	7.11	0.10	2.81	5.76	3.27	0.72	0.04	0.06	6.99	99.80
16R-1, 135–138 cm	305.95	62.21	0.29	15.16	6.52	0.10	1.96	5.55	3.71	0.66	0.04	0.00	3.43	99.61
16R-2, 12–17 cm	306.22	58.79	0.31	16.05	7.30	0.11	2.74	5.79	3.46	0.72	0.03	0.01	4.84	100.14
17R-1, 67–69 cm	314.97	58.51	0.32	17.21	7.60	0.09	1.98	6.37	4.34	0.49	0.17	0.02	2.88	99.96
19R-1, 10–17 cm	333.70	56.26	0.28	16.61	7.37	0.12	4.13	7.25	3.02	0.62	0.03	0.01	4.35	100.03
20R-1, 43–46 cm	343.73	51.86	0.22	12.09	8.03	0.18	11.76	8.06	2.05	0.35	0.01	0.01	5.08	99.69
20R-1, 72–74 cm	344.02	52.16	0.22	12.36	8.13	0.18	10.57	7.95	2.03	0.34	0.00	0.01	5.77	99.70
20R-1, 124–128 cm	344.54	58.92	0.29	16.24	6.89	0.10	2.39	6.11	3.75	0.48	0.07	0.08	4.76	100.04
21R-1, 26–30 cm	353.26	57.25	0.30	16.78	6.87	0.07	1.65	6.35	4.10	0.82	0.32	0.02	5.21	99.71
21R-2, 28–32 cm	354.70	65.18	0.24	13.04	3.59	0.08	0.84	2.53	3.84	2.25	0.07	0.00	7.59	99.22
21R-2, 103–107 cm	355.46	51.89	0.21	12.00	7.90	0.15	10.06	8.78	2.40	0.25	0.04	0.00	6.02	99.67
24R-1, 41–45 cm	383.31	66.77	0.31	14.80	5.07	0.08	1.37	4.29	4.66	0.96	0.11	0.00	1.10	99.50
24R-2, 5–9 cm	383.45	65.19	0.30	14.67	5.20	0.08	1.49	4.44	4.30	1.02	0.06	0.00	2.62	99.36
25R-1, 64–72 cm	392.14	66.09	0.32	15.32	5.07	0.08	1.28	4.52	4.82	1.08	0.20	0.00	0.95	99.70
27R-1, 31–35 cm	411.11	64.10	0.29	13.94	4.79	0.07	1.39	3.91	4.30	0.92	0.06	0.00	5.45	99.21
28R-1, 15–18 cm	420.55	57.93	0.16	12.82	7.03	0.13	8.72	7.36	2.63	0.43	0.02	0.00	2.62	99.83
29R-1, 63–66 cm	430.73	49.11	0.20	11.17	7.59	0.19	10.12	12.21	2.02	0.18	0.19	0.00	7.08	100.02
30R-1, 7–9 cm	439.77	56.71	0.23	13.33	6.52	0.11	7.79	7.83	2.96	0.55	0.08	0.01	3.39	99.50
30R-2, 39–45 cm	441.59	57.75	0.21	13.39	6.39	0.11	4.81	8.26	3.39	0.81	0.04	0.00	4.82	99.96
30R-2, 136–139 cm	442.63	51.08	0.38	14.27	8.26	0.17	9.79	8.93	2.29	0.25	0.06	0.01	4.65	100.11
31R-1, 102–109 cm	450.42	59.12	0.21	13.69	6.16	0.08	5.99	6.99	3.35	0.60	0.04	0.00	3.72	99.94
34R-4, 14–20 cm	482.84	51.85	0.19	11.22	7.65	0.12	8.86	9.42	2.45	0.57	0.02	0.00	6.47	98.80
35R-1, 127–130 cm	489.29	54.88	0.29	12.40	4.78	0.07	2.00	11.71	3.33	1.05	0.08	0.04	8.70	99.32
35R-2, 1–7 cm	489.51	62.96	0.28	14.65	5.30	0.05	2.74	4.79	4.38	0.50	0.06	0.01	4.09	99.79
36R-1, 52–59 cm	498.22	69.32	0.27	13.22	3.92	0.03	1.50	3.20	4.66	1.04	0.09	0.01	2.60	99.84
37R-3, 13–15 cm	510.45	54.21	0.25	13.91	7.82	0.09	8.05	7.87	2.69	0.38	0.04	0.05	4.41	99.77
38R-1, 76–83 cm	517.86	55.72	0.24	14.89	7.39	0.10	3.06	5.13	3.17	1.06	0.02	0.32	8.74	99.82
39R-1, 47–53 cm	527.27	60.17	0.27	16.65	6.36	0.07	2.37	6.90	3.74	0.43	0.09	0.00	2.87	99.92
39R-2, 119–123 cm	529.49	60.51	0.34	14.61	7.73	0.11	2.64	6.24	3.46	0.78	0.04	0.02	3.51	99.97
40R-2, 83–90 cm	538.41	47.89	0.27	12.24	8.04	0.15	9.39	11.69	2.06	0.29	0.02	0.00	8.00	100.04
42R-2, 15–21 cm	557.25	57.46	0.23	14.61	5.76	0.07	6.28	6.81	3.44	0.82	0.06	0.03	4.50	100.07
42R-4, 46–54 cm	560.51	58.85	0.21	13.75	6.23	0.08	6.16	6.39	3.27	0.58	0.04	0.02	4.30	99.86
43R-2, 43–52 cm	566.73	55.97	0.21	13.64	6.00	0.09	5.60	7.84	3.37	0.62	0.03	0.00	6.11	99.49
43R-2, 100–105 cm	567.30	57.35	0.22	13.70	6.32	0.09	6.03	6.90	3.27	0.73	0.04	0.04	5.32	99.99
44R-1, 38–45 cm	574.98	50.40	0.29	12.61	8.63	0.19	11.41	7.66	2.27	0.34	0.03	-0.01	6.15	99.94
44R-1, 102–109 cm	575.62	49.61	0.28	12.09	8.46	0.21	12.24	7.44	2.14	0.33	0.02	-0.01	7.30	00.09

removal and/or addition of these phases within and between specific groups as causes of major-element variations.

For example, plots of (0.5 (Mg + Fe))/(K or Ti) vs. Si/(K or Ti) and (Ca + 0.5 (Na - Al)/(K or Ti) vs. Al/(K or Ti) (in which K and Ti are assumed to be incompatible, conserved elements) help to discriminate between fractionation of the various ferromagnesian silicates and clinopyroxene-plagioclase, respectively (Fig. 8) (Stanley and Russell, 1989). Vectors can be constructed on these plots that reflect the stoichiometry of specific phases, according to the proportions of the various atomic components. For example, olivine removal from or addition to a melt can be detected with the aid of a plot of 0.5(Mg + Fe)/K vs. Si/K (Figs. 8A, 8B, 8C, 8D). Analytical data for samples related by olivine subtraction/addition alone will project on a vector with a slope equal to unity, and similar vectors can be constructed for other probable fractionating phases.

A few features of these plots are particularly noteworthy:

1. In the case of Figures 8A and 8B, clearly (a) the boninite groups (1–3) have experienced similar proportions of olivine-pyroxene fractionation; (b) Clinopyroxene is volumetrically important in these fractionation processes; (c) the larger spread of data with K as a denominator (8A) compared with Ti (8B) probably relates to alteration effects. Note that the LCB appear to define a trend in Figure 8A that projects through zero (a K-alteration vector) whereas the ICB group does not define such a trend; (d) the HCB group can be clearly divided into two groups on the basis of either Figure 8A or 8B. The samples projected at low 0.5(Mg + Fe)/K (or Ti) values are from three sills intruded at relatively shallow levels in Hole 786B (lithological subunits 2, 9, and 19, respectively); (e) In Figure 8B, all groups give non-zero intercepts, and different but sub-parallel slopes corresponding to the observed mineral assemblage of olivine + orthopyroxene. The compositional spread can be accounted for by the existence of distinct primary magma compositions with superimposed fractionation and crystal accumulation.

2. In comparison with progressive partial melting vectors (Figs. 8C and 8D) derived from an experimental study of the dry melting behavior of depleted spinel lherzolite (Tinaquillo peridotite) (Jaques and Green, 1980), it is clear that (a) the incongruent melting behavior of orthopyroxene in the source of the boninite groups results in a shift of projected compositions away from the Tinaquillo trajectory to

Table 2 (continued).

Sample	Depth (mbsf)	SiO_2	TiO_2	Al_2O_3	Fe_2O_3*	MnO	MgO	CaO	Na_2O	K_2O	P_2O_5	S	LOI	Total
125-786B-														
45R-1, 41–49 cm	584.71	60.14	0.32	14.55	7.19	0.11	4.71	6.58	3.37	0.66	0.04	0.00	2.52	100.17
46R-1, 39–43 cm	594.29	56.95	0.39	14.58	7.16	0.13	5.22	6.63	3.32	0.73	0.06	0.01	4.52	99.69
46R-1, 119–125 cm	595.09	58.00	0.40	14.63	7.22	0.13	5.12	6.68	2.98	0.86	0.10	0.01	2.91	99.00
46R-2, 54–58 cm	595.94	55.40	0.35	14.32	7.11	0.13	5.81	6.21	2.87	0.56	0.04	0.01	6.70	99.49
47R-1, 18–22 cm	603.68	56.37	0.32	14.66	7.37	0.15	5.76	7.14	2.95	0.61	0.04	0.01	4.50	99.86
47R-1, 112–116 cm	604.62	50.31	0.31	14.33	7.45	0.15	6.46	6.09	2.71	0.87	0.02	0.02	11.20	99.90
48R-1, 48–53 cm	613.68	47.43	0.38	16.58	9.55	0.09	4.34	8.59	3.55	0.97	1.48	0.04	6.90	99.88
49R-2, 99–103 cm	624.95	51.42	0.37	14.10	7.54	0.17	6.36	5.93	2.87	0.86	0.05	0.02	10.00	99.65
50R-1, 137–141 cm	633.87	55.54	0.30	13.48	7.42	0.13	6.75	5.99	2.76	0.54	0.04	0.02	6.76	99.72
50R-2, 45–48 cm	635.86	57.39	0.31	12.63	7.20	0.14	8.69	6.17	2.85	0.50	0.05	0.01	3.74	99.68
51R-1, 49–56 cm	642.69	53.98	0.20	12.67	8.09	0.15	10.77	7.51	2.29	0.35	0.16	0.03	3.91	100.11
51R-2, 5–9 cm	643.75	52.10	0.29	12.53	8.28	0.17	11.01	7.45	2.30	0.26	0.18	0.03	4.77	99.37
52R-1, 112–116 cm	653.02	50.25	0.23	11.44	7.71	0.15	9.01	4.79	2.05	0.68	0.02	0.01	13.00	99.32
53R-1, 66–72 cm	662.26	52.64	0.25	11.21	7.81	0.30	8.18	7.36	2.24	0.49	0.04	0.01	8.92	99.42
53R-1, 82–85 cm	662.42	55.95	0.27	12.35	7.28	0.23	8.35	7.56	2.35	0.50	0.06	0.01	4.35	99.23
54R-1, 50–54 cm	671.70	52.85	0.25	11.29	7.19	0.15	9.47	7.12	2.15	0.40	0.03	0.01	8.85	99.76
54R-2, 26–30 cm	672.96	54.01	0.24	11.67	7.28	0.14	9.29	5.71	2.18	0.45	0.04	0.02	9.15	100.15
54R-2, 84–88 cm	673.54	55.13	0.26	12.28	8.19	0.15	9.62	6.74	2.27	0.58	0.04	0.02	4.85	100.11
54R-2, 144–147 cm	674.14	54.86	0.25	11.94	7.25	0.13	8.93	5.92	2.17	0.43	0.04	0.01	7.73	99.65
54R-3, 60–65 cm	674.80	54.95	0.27	11.93	7.38	0.14	9.29	5.78	1.88	0.46	0.04	0.01	7.35	99.46
54R-4, 75–79 cm	676.45	54.82	0.26	12.13	7.19	0.13	9.07	5.82	2.09	0.45	0.04	0.01	7.81	99.78
54R-5, 8–15 cm	676.98	55.24	0.27	11.99	7.45	0.13	8.92	5.96	2.06	0.42	0.04	0.01	6.81	99.27
55R-1, 87–91 cm	681.67	55.98	0.32	12.06	7.83	0.25	7.51	7.24	2.30	0.59	0.05	0.02	5.31	99.43
55R-2, 11–16 cm	682.31	55.73	0.27	12.17	7.28	0.15	7.64	6.57	2.20	0.53	0.04	0.01	6.92	99.49
55R-3, 44–49 cm	684.09	52.60	0.28	10.56	7.07	0.16	11.26	4.36	1.94	0.38	0.04	0.01	10.90	99.53
56R-2, 51–56 cm	692.11	50.59	0.20	10.74	7.17	0.11	11.64	4.45	2.54	1.14	0.01	0.00	11.00	99.57
57R-2, 124–128 cm	702.46	47.37	0.21	10.39	8.90	0.18	13.11	3.97	2.68	0.81	0.05	0.01	12.41	100.09
57R-4, 69–77 cm	704.70	50.28	0.19	10.90	7.39	0.13	12.19	4.90	2.89	0.48	0.01	0.00	10.50	99.84
58R-1, 116–120 cm	710.56	53.97	0.24	10.50	7.59	0.12	11.52	5.12	3.29	0.07	0.04	0.02	7.12	99.59
58R-3, 62–69 cm	712.83	57.31	0.17	9.98	6.45	0.12	10.03	4.63	3.52	0.10	0.03	0.00	7.25	99.56
59R-3, 84–91 cm	717.92	52.28	0.18	10.46	7.82	0.13	13.01	4.94	3.44	0.06	0.03	0.00	7.46	99.78
60R-3, 102–108 cm	722.77	57.02	0.17	10.01	6.68	0.12	10.76	4.83	3.55	0.14	0.02	0.00	6.55	99.82
61R-4, 96–102 cm	733.96	68.54	0.31	12.94	4.48	0.07	0.54	3.41	4.68	1.66	0.08	0.00	2.93	99.62
62R-1, 114–120 cm	739.54	55.77	0.17	9.67	6.48	0.08	10.92	3.48	2.99	0.40	0.02	0.07	9.58	99.61
63R-2, 86–91 cm	750.36	74.63	0.22	11.92	2.44	0.04	0.29	1.38	3.26	3.49	0.05	0.07	0.93	98.70
64R-2, 93–105 cm	760.03	71.55	0.23	12.34	3.73	0.05	0.96	1.68	3.32	4.00	0.05	0.01	1.68	99.60
65R-1, 21–25 cm	767.61	54.53	0.40	17.18	7.20	0.09	5.45	6.45	3.37	0.49	0.05	0.00	4.95	100.14
65R-2, 5–12 cm	768.95	71.57	0.24	12.98	3.65	0.05	1.26	1.10	3.61	3.70	0.06	0.04	1.48	99.72
66R-1, 26–33 cm	777.36	69.93	0.24	13.10	3.87	0.07	1.24	2.17	3.60	2.89	0.06	0.07	2.51	99.73
66R-3, 18–24 cm	780.23	72.04	0.23	12.80	3.26	0.06	0.95	0.84	3.18	4.61	0.06	0.02	1.34	99.36
67R-1, 33–41 cm	787.03	75.33	0.23	12.40	2.58	0.03	0.40	1.18	4.21	2.69	0.05	0.00	0.69	99.77
69R-1, 68–77 cm	797.98	59.45	0.21	11.47	5.57	0.07	7.63	3.04	3.77	0.13	0.04	0.65	7.89	99.91
69R-4, 105–113 cm	802.36	56.94	0.21	11.30	5.87	0.12	7.74	4.50	3.58	0.10	0.04	0.70	8.98	100.06
69R-5, 60–64 cm	803.07	58.96	0.19	10.89	6.59	0.09	7.63	3.64	3.13	0.07	0.03	1.44	7.90	100.55
69R-7, 34–42 cm	805.68	56.25	0.20	11.19	6.23	0.12	8.22	4.00	3.82	0.14	0.03	0.10	9.81	100.11
70R-1, 92–96 cm	807.82	55.64	0.24	10.50	6.08	0.17	7.79	5.39	3.06	0.18	0.05	0.12	10.16	99.34
70R-2, 5–11 cm	808.45	56.27	0.20	10.98	6.08	0.15	7.41	5.78	3.09	0.26	0.03	0.05	9.32	99.60
70R-4, 11–17 cm	811.32	54.05	0.24	13.02	7.32	0.09	9.65	2.80	2.57	0.38	0.03	1.56	8.12	99.82
71R-4, 7–12 cm	819.99	57.69	0.24	14.29	5.88	0.08	7.70	4.18	2.78	0.40	0.03	0.54	6.15	99.93
71R-4, 74–80 cm	820.66	57.34	0.22	13.81	5.93	0.06	6.73	5.07	3.16	0.10	0.03	0.72	6.97	100.13
71R-4, 141–146 cm	812.33	56.45	0.22	13.34	6.76	0.06	6.63	5.29	3.11	0.08	0.03	1.53	6.97	100.45
72R-1, 3–7 cm	823.63	56.79	0.30	14.22	6.63	0.05	7.71	1.39	2.99	0.86	0.05	2.40	7.43	100.81

lower Mg + Fe/K or Ti and higher Si/K or Ti; (b) the residual mineralogy for all of the boninite groups included orthopyroxene (note the melting vector determined by Jaques and Green (1980) steepens at higher percentages of melting, becoming dominated by an olivine control line).

3. A K-alteration vector is apparent for both the LCBrzA and the LCB groups (Fig. 8E), but the offset and subparallel trends for these two groups (Fig. 8F) are not simply accounted for by fractionation/accumulation of the observed phenocryst phases.

4. In contrast, the ICBrzA do not appear to have been affected by K-addition/loss (compare Figs. 8G and 8H). Relationships among the ICB and ICBrzA postulated by van der Laan et al. (this volume) are depicted on these figures. It is possible that the ICBrzA projected at low Si/K or Si/Ti values are derivative melts (by fractional crystallization of olivine-orthopyroxene-clinopyroxene-plagioclase) of parental ICB compositions, and that the ICBrzA projected at high Si/Ti represent cumulus-enriched types.

5. More extensive K-loss in the ICBrzA compared with A, D, and R compositions is shown in Figure 8I. Nevertheless, K-alteration is also apparent for the R group, consistent with the alteration observed in the cores (Fig. 8J). From the equivalent type of plot (Fig. 8K) with Ti as denominator, the following inferences can be drawn (a) the A, D, and R groups may be related by fractional crystallization of pyroxene-plagioclase-magnetite assemblages. However, (b) overlap of the A with the low Si/Ti portion of the ICBrzA compositional spectrum could be interpreted as resulting from cumulus enrichment of the andesitic compositions and furthermore, (c) changes in the relative proportions of pyroxene-plagioclase-magnetite through the bronzite andesite-rhyolite sequence is indicated, and the considerable scatter evident as a whole suggests multiple lineages were involved.

In summary, the detailed inter-relationships of the rock groups encountered in Site 786 are complex, and simple fractional crystallization histories alone are clearly inappropriate. The eruption of magmas with

Table 2 (continued).

Sample	Nb	Zr	Y	Sr	Rb	Th	Pb	U	Ga	Zn	Cu	Ni	Cr	Ce	Nd	Ba	V	La	Sc
125-786B-																			
1R-1, 25–28 cm																			
1R-1, 75–79 cm																			
1R-1, 89–93 cm	1	40	7	167	8	0	2	1	9	58	62	96	471	1	0	54	153	4	24
2R-1, 72–76 cm	1	42	6	165	7	0	1	1	8	58	68	91	471	6	0	48	152	3	27
3R-1, 34–44 cm	0	41	6	168	8	2	3	1	9	59	65	91	456	0	0	63	150	5	30
4R-1, 109–111 cm	0	44	6	170	7	2	2	2	11	60	74	85	405	6	2	67	163	6	25
5R-1, 23–25 cm																			
5R-2, 1–6 cm	1	49	9	198	7	0	2	0	12	64	55	64	238	8	2	58	157	4	22
6R-3, 17–22 cm	0	31	10	129	3	0	0	2	11	67	54	202	564	0	0	11	229	3	32
8R-1, 43–44 cm																			
9R-1, 15–17 cm																			
11R-1, 103–108 cm	1	39	5	174	5	0	0	0	12	71	41	149	580	10	1	50	153	5	32
12R-2, 124–126 cm	0	35	6	157	6	3	3	2	9	65	58	127	564	0	0	42	184	5	40
13R-2, 134–138 cm	1	37	6	178	7	0	1	3	9	57	65	116	473	0	0	45	169	5	26
15R-2, 3–8 cm	1	56	12	217	7	2	1	3	16	78	75	17	8	9	5	42	203	4	20
16R-1, 135–138 cm																			
16R-2, 12–17 cm	1	57	9	217	9	1	0	0	14	80	80	17	15	1	0	39	205	7	28
17R-1, 67–69 cm	1	61	35	248	6	3	4	2	17	76	69	13	10	16	10	77	219	11	23
19R-1, 10–17 cm	0	49	11	210	6	1	3	1	13	79	82	38	67	2	0	20	202	2	27
20R-1, 43–46 cm																			
20R-1, 72–74 cm																			
20R-1, 124–128 cm	1	57	21	217	6	2	3	3	13	72	83	22	12	7	5	61	197	9	29
21R-1, 26–30 cm	0	56	28	233	13	3	4	1	16	59	78	16	17	19	4	54	190	10	21
21R-2, 28–32 cm	1	79	12	128	30	0	2	1	10	54	61	13	3	9	4	68	19	7	15
21R-2, 103–107 cm	1	28	7	133	5	2	4	2	10	71	63	275	1004	3	0	25	165	3	31
24R-1, 41–45 cm	1	71	15	199	13	4	3	0	15	49	49	7	14	6	2	80	153	7	19
24R-2, 5–9 cm	1	67	10	189	10	3	5	1	9	55	97	8	15	6	1	69	183	4	13
25R-1, 64–72 cm	0	72	12	207	12	1	2	1	14	48	40	6	7	9	1	68	163	6	13
27R-1, 31–35 cm																			
28R-1, 15–18 cm	0	33	5	192	6	3	2	2	8	58	62	134	491	4	0	36	153	4	31
29R-1, 63–66 cm	0	25	5	138	5	1	1	1	8	76	34	245	956	4	0	53	160	6	36
30R-1, 7–9 cm	1	33	5	207	9	1	2	1	11	65	29	136	524	7	4	56	166	2	31
30R-2, 39–45 cm	1	29	5	129	15	1	1	1	8	48	13	92	513	4	0	64	141	4	33
30R-2, 136–139 cm	1	32	10	130	4	3	2	1	13	65	57	188	552	5	0	3	231	4	35
31R-1, 102–109 cm	0	42	7	174	10	0	0	2	11	57	29	129	585	4	0	82	160	6	26
34R-4, 14–20 cm	1	26	6	128	15	1	1	3	7	48	47	246	930	2	0	38	145	4	35
35R-1, 127–130 cm	1	52	9	173	31	4	4	0	12	55	22	17	53	9	6	55	98	4	26
35R-2, 1–7 cm	1	62	10	201	8	1	0	3	12	64	58	19	43	5	1	80	121	5	16
36R-1, 52–59 cm	1	70	13	171	22	3	1	1	12	51	21	5	14	6	1	80	56	3	12
37R-3, 13–15 cm	0	30	9	153	14	2	5	1	12	69	21	193	724	0	0	38	196	3	31
38R-1, 76–83 cm	1	43	6	261	21	3	2	2	13	58	84	53	10	7	1	58	196	2	16
39R-1, 47–53 cm	0	47	11	236	5	1	0	3	14	112	32	14	11	4	2	53	238	6	24
39R-2, 119–123 cm	1	48	11	173	16	2	1	1	13	67	108	15	11	8	3	54	270	4	26
40R-2, 83–90 cm	0	23	8	131	7	1	1	2	10	59	34	349	961	3	0	25	187	2	38
42R-2, 15–21 cm	0	42	8	191	9	1	3	2	14	52	39	88	387	4	0	66	171	8	27
42R-4, 46–54 cm	1	40	6	179	8	1	1	0	11	52	44	90	356	4	0	64	166	3	25
43R-2, 43–52 cm	1	31	6	140	7	1	1	1	9	36	10	68	272	1	0	46	117	3	18
43R-2, 100–105 cm	0	41	7	183	7	1	0	2	11	55	10	94	382	0	0	55	161	3	30
44R-1, 38–45 cm	0	26	8	117	7	1	0	1	11	62	44	315	804	0	0	23	190	0	28
44R-1, 102–109 cm	0	26	7	107	8	1	0	1	9	67	157	367	915	4	3	38	193	4	26

marked cumulus enrichments is inferred. Given the widespread impression that plagioclase is insignificant in the evolution of boninite systems, it is important to realize that evidence from this site stands in stark contradiction (Figs. 8L and 8M). In terms of the probable cumulate assemblages at depth, we predict that noritic gabbros must be volumetrically significant and may well be represented in the pervasive glomeroporphyritic and corroded plagioclase-pyroxene clusters in volcanic rocks of the site (van der Laan et al., this volume).

Bonin-Mariana Forearc Comparisons

To a first approximation, many overall geochemical similarities exist between the boninite and related rock suites of Site 786 and the rocks of comparable age from Chichijima, Sites 782 and 793, also located in the Bonin forearc, Guam (Facpi and Alutom Formations), and the Mariana Forearc (Umino, 1986; Shipboard Scientific Party, 1990a; Shipboard Scientific Party 1990c; Reagan and Meijer, 1984; Bloomer and Hawkins, 1987; Wood et al., 1981). By way of comparison, representative compositional data from these locations are shown in the major-element plots of Figure 9. Some important features that emerge from these plots are as follows:

1. A remarkable along-strike occurrence of boninite-related rocks has now been documented in the forearc of the Bonin-Mariana system from at least 32° to 11° N, but within and between boninite locations other rock types of similar age are present.

2. The intermediate- and low-Ca boninites and bronzite andesites (Groups 2, 3, 4, and 5) of Site 786 and the type boninites of Chichijima may be distinctive on the basis of high MgO at specific SiO_2 content, and generally have lower TiO_2 than rock types from these other Bonin-Mariana forearc locations.

3. The younger (early to late Oligocene and possibly middle Miocene) rocks from Sites 786 (e.g., the high-Ca boninite of Group 1), 793, and the Alutom Formation of Guam appear to have generally higher TiO_2 contents than the older (middle Eocene) units.

We interpret the low TiO_2 contents to reflect the overall refractory (melt-depleted) character of the upper mantle source involved in magma genesis and conclude that Site 786 and Chichijima represent

Table 2 (continued).

Sample	Nb	Zr	Y	Sr	Rb	Th	Pb	U	Ga	Zn	Cu	Ni	Cr	Ce	Nd	Ba	V	La	Sc
125-786B-																			
45R-1, 41–49 cm	1	45	9	172	10	0	0	2	13	62	100	56	193	4	0	68	228	4	24
46R-1, 39–43 cm	1	46	13	177	9	2	3	0	13	62	76	61	178	6	5	46	264	6	27
46R-1, 119–125 cm	0	47	10	178	10	2	3	0	13	61	89	60	185	4	4	52	242	8	23
46R-2, 54–58 cm	1	45	10	170	9	3	6	0	13	66	73	65	183	11	4	24	236	5	28
47R-1, 18–22 cm	0	41	8	173	8	2	4	0	14	65	68	70	247	7	4	65	215	7	26
47R-1, 112–116 cm	1	41	5	156	15	3	6	2	13	60	93	72	230	3	3	27	118	9	29
48R-1, 48–53 cm	0	47	95	233	37	4	4	2	25	104	86	47	166	58	20	48	269	32	33
49R-2, 99–103 cm	1	42	8	188	15	3	3	0	13	64	88	90	189	5	2	41	195	8	23
50R-1, 137–141 cm	0	40	7	150	9	1	2	0	12	60	112	108	395	1	1	27	171	3	23
50R-2, 45–48 cm	0	38	6	155	9	3	4	1	11	60	70	184	763	1	1	62	169	4	25
51R-1, 49–56 cm	1	33	17	151	5	0	0	0	11	67	44	196	921	14	6	56	212	7	31
51R-2, 5–9 cm	0	34	18	152	3	5	6	1	11	69	56	197	887	13	6	35	211	7	33
52R-1, 112–116 cm	1	33	2	108	14	3	16	2	11	87	92	172	687	4	1	42	92	5	27
53R-1, 66–72 cm	0	31	6	131	12	2	4	1	12	57	72	252	697	1	4	59	146	3	26
53R-1, 82–85 cm	1	34	7	146	8	4	5	2	13	60	57	163	799	5	4	38	186	3	32
54R-1, 50–54 cm	1	32	5	153	8	4	2	1	10	56	53	217	767	9	2	59	150	4	29
54R-2, 26–30 cm	1	33	6	123	8	3	5	1	11	58	55	163	799	5	0	41	160	2	30
54R-2, 84–88 cm	1	34	8	141	9	4	4	2	11	62	46	185	840	11	4	43	179	4	33
54R-2, 144–147 cm	0	33	4	125	7	1	4	2	9	60	55	151	848	7	4	37	179	1	29
54R-3, 60–65 cm	0	34	6	127	9	5	5	1	11	62	58	160	821	6	2	74	170	2	26
54R-4, 75–79 cm	0	36	6	137	9	5	5	2	10	59	47	154	667	6	2	37	176	4	31
54R-5, 8–15 cm	1	34	6	134	10	3	3	1	11	60	114	163	722	5	2	43	158	5	26
55R-1, 87–91 cm	1	34	6	148	11	2	3	1	11	58	74	173	694	11	2	172	180	2	31
55R-2, 11–16 cm	2	36	5	144	10	5	4	0	11	59	47	161	674	9	2	35	179	3	25
55R-3, 44–49 cm	0	30	6	96	8	4	4	2	9	57	75	217	949	8	3	33	158	7	30
56R-2, 51–56 cm	1	30	4	119	15	4	4	2	11	55	33	197	949	0	0	69	144	5	27
57R-2, 124–128 cm	1	29	7	107	12	3	4	0	11	72	18	341	1014	7	0	14	135	7	27
57R-4, 69–77 cm	0	30	4	106	9	1	1	1	9	61	18	281	1200	5	0	27	134	3	29
58R-1, 116–120 cm	0	29	7	91	1	4	6	1	12	56	26	281	1065	3	4	29	186	1	26
58R-3, 62–69 cm	0	25	6	83	3	0	1	2	8	50	50	247	1017	1	0	20	192	3	27
59R-3, 84–91 cm	1	29	6	91	0	1	1	2	9	61	29	289	1128	0	0	30	144	1	28
60R-3, 102–108 cm	0	26	5	80	2	1	1	0	11	53	43	271	999	0	0	21	203	5	25
61R-4, 96–102 cm	0	81	15	123	28	2	3	2	13	57	32	4	8	9	5	175	38	6	12
62R-1, 114–120 cm	1	28	7	88	6	2	2	0	9	58	145	269	977	2	1	55	121	4	27
63R-2, 86–91 cm	1	71	10	93	32	1	1	1	7	86	31	4	14	15	2	679	27	4	13
64R-2, 93–105 cm	1	72	12	77	37	3	3	2	9	67	30	11	22	11	3	756	33	3	13
65R-1, 21–25 cm	1	44	10	160	5	3	2	2	15	75	67	21	18	5	0	56	241	4	29
65R-2, 5–12 cm	1	75	11	91	34	1	0	1	10	63	76	7	18	10	6	673	31	5	10
66R-1, 26–33 cm	0	75	10	108	28	2	4	1	11	92	54	5	15	11	5	325	29	4	16
66R-3, 18–24 cm	0	73	9	76	44	0	0	2	10	77	53	4	17	13	5	708	32	5	13
67R-1, 33–41 cm	1	77	12	102	24	1	1	1	8	105	38	3	11	7	2	430	22	4	14
69R-1, 68–77 cm	0	46	8	123	2	0	5	2	11	110	65	159	676	6	2	58	121	7	21
69R-4, 105–113 cm	0	43	7	126	2	0	5	1	11	60	68	177	728	3	2	43	123	5	20
69R-5, 60–64 cm	0	40	7	130	1	0	11	2	9	70	199	216	787	5	2	55	124	3	27
69R-7, 34–42 cm	1	42	7	114	1	3	1	0	10	83	90	195	765	3	0	7	123	5	28
70R-1, 92–96 cm	1	42	8	122	1	3	6	0	11	88	75	196	761	7	1	73	118	3	23
70R-2, 5–11 cm	0	42	7	133	3	1	1	3	9	65	66	191	786	8	2	45	122	7	24
70R-4, 11–17 cm	0	34	6	104	3	0	2	2	11	65	80	212	811	3	0	54	205	2	29
71R-4, 7–12 cm	1	40	7	136	3	0	2	1	13	107	61	120	510	4	0	58	186	4	27
71R-4, 74–80 cm	1	38	7	164	1	2	4	2	11	139	72	109	506	0	0	26	193	5	26
71R-4, 141–146 cm	0	38	5	162	0	0	6	3	10	101	304	180	535	3	1	25	194	4	32
72R-1, 3–7 cm	0	37	7	142	8	1	3	1	10	39	22	183	805	4	3	66	182	4	32

* All Fe reported as Fe_2O_3.

the extreme of this depleted source type in the western Pacific. As a measure of the degree of relative depletion of respective upper mantle sources, the variation of refractory lithophile oxides in the different suites is shown in Figure 10. The concentrations of these magmaphile oxides are unlikely to have been affected by subduction zone-derived fluids, and reflect the prior melt extraction history of sources in the upper mantle. A spread from MORB-like values for some of the tholeiitic andesites from Site 458 to extremely high Al_2O_3/TiO_2 at low TiO_2 for Site 786 and Chichijima rocks can be observed. The remarkable features of this kind of plot are the very low absolute TiO_2 concentrations and high Al_2O_3/TiO_2 values of the boninitic suites of the western Pacific compared with MORB, given the fact that MORB themselves represent melts derived from relatively refractory upper mantle source lithologies.

An additional feature, however, of these boninite-related suites is the clear evidence for along-strike variations in the detailed characteristics of the primary upper mantle sources, the nature of mantle metasomatic events prior to melt production (see Pearce et al., this volume), and possible variations in the physical conditions prevailing during melting.

A comparison of the boninite and bronzite andesite groups present at Site 786 with other boninite types recognized by Crawford et al. (1989) is shown in Figure 6. As mentioned previously, the Site 786 suite spans the chemical variation documented globally for these boninite types. The postulated relationships (Crawford et al., 1989) among these boninite types is as follows:

1. Production of low-Ca Type 3 boninites (e.g., those from the Chichijima-type locality and Cape Vogel in Papua New Guinea) by hydrous fluid-fluxed melting of hot (T > 1200° C), refractory harzburgite.

2. More extensive metasomatic flux (involving perhaps both slab-derived and hot-spot-related melts) to even more refractory harzburgite prior to generation of low-Ca Type 1 boninites (e.g., Nepoui, New Caledonia).

Table 3. Major- and trace-element analyses obtained on board with modifications as described in the text, of representative lithologies from Site 786.

Sample	Depth (mbsf)	SiO_2	TiO_2	Al_2O_3	Fe_2O_3*	MnO	MgO	CaO	Na_2O	K_2O	P_2O_5	LOI	Total
125-786A-													
6X-5, 24–27 cm	109.94	52.72	0.83	16.26	12.34	0.20	4.14	9.73	1.04	0.35	0.00	0.85	98.14
12X-1, 140–142 cm	107.10	53.03	0.30	17.81	8.60	0.09	5.20	8.46	1.89	1.42	0.00	3.01	96.84
13X-CC, 27–29 cm	115.57	55.71	0.17	12.91	8.41	0.01	13.57	5.84	1.39	0.88	0.00	6.15	98.99
16X-CC, 25–28 cm	145.19	52.29	0.22	14.99	8.01	0.10	11.82	8.26	1.61	0.33	0.00	2.47	97.65
17X-CC, 4–6 cm	154.04	51.90	0.14	12.19	9.84	0.20	15.33	7.02	1.85	0.75	0.00	6.57	99.23
19X-1, 0–30 cm	164.17	52.47	0.21	14.93	8.06	0.11	11.36	8.33	1.39	0.53	0.00	4.89	97.39
19X-CC, 17–20 cm	164.19	50.17	0.23	11.30	9.47	0.17	19.89	6.08	1.08	0.43	0.00	5.50	98.86
125-786B-													
1R-1, 61–64 cm	163.11	61.48	0.14	12.67	7.19	0.11	7.98	6.23	2.10	0.52	0.00	2.24	98.48
2R-1, 58–61 cm	170.08	62.18	0.15	12.63	6.94	0.11	7.20	6.20	2.12	0.56	0.00	2.09	98.10
3R-1, 94–97 cm	180.14	58.97	0.16	13.62	7.68	0.11	8.89	5.52	1.52	0.83	0.00	3.93	97.28
5R-2, 70–72 cm	200.80	52.05	0.29	14.92	8.86	0.11	7.95	11.28	1.63	1.30	0.01	3.52	97.36
6R-2, 128–130 cm	210.98	52.47	0.29	14.40	8.74	0.17	11.14	9.50	1.13	0.26	0.00	1.94	98.08
8R-1, 45–47 cm	228.05	55.93	0.24	17.98	7.98	0.12	4.09	7.91	2.44	0.67	0.00	2.79	97.34
9R-1, 10–15 cm	237.20	57.25	0.25	17.42	7.58	0.11	3.91	7.68	2.11	0.58	0.00	2.01	96.88
11R-1, 122–126 cm	257.52	55.22	0.14	13.27	7.84	0.14	11.20	6.69	1.23	0.43	0.00	2.88	97.64
12R-2, 14–16 cm	267.57	55.48	0.16	14.01	8.47	0.15	11.80	7.33	1.31	0.32	0.00	2.21	98.51
12R-2, 120–124 cm	268.63	60.18	0.12	12.98	7.22	0.12	8.51	6.83	1.58	0.45	0.03	1.55	97.99
16R-1, 137–141 cm	305.97	63.45	0.26	15.32	6.92	0.09	1.65	5.63	2.93	0.74	0.00	2.54	96.99
19R-1, 91–94 cm	334.51	59.55	0.22	16.65	7.67	0.12	3.66	7.31	2.05	0.73	0.00	2.40	97.96
21R-1, 26–29 cm	353.26	58.61	0.28	17.48	7.94	0.10	1.91	6.76	2.89	0.88	0.04	3.00	96.88
21R-1, 129–131 cm	354.29	71.70	0.20	13.52	3.74	0.07	0.33	2.47	3.11	2.20	0.00	6.97	97.30
21R-2, 72–76 cm	355.20	53.80	0.16	12.54	8.65	0.15	6.14	14.17	1.27	0.41	0.00	6.11	97.27
22R-3, 61–64 cm	370.00	72.06	0.19	13.21	3.58	0.07	0.12	2.14	3.90	2.59	0.02	8.68	97.06
24R-1, 9–12 cm	381.99	66.46	0.26	14.92	5.20	0.07	0.89	4.48	3.43	0.82	0.02	0.44	96.52
26R-1, 68–70 cm	401.88	66.45	0.26	14.64	4.76	0.06	0.55	3.82	3.60	1.14	0.00	0.31	96.76
30R-1, 29–31 cm	439.99	58.56	0.09	12.75	7.29	0.09	6.81	10.27	1.79	0.91	0.00	4.42	98.04
30R-1, 119–121 cm	440.89	60.64	0.15	13.41	6.62	0.09	5.83	8.36	2.14	0.73	0.00	3.55	97.94
31R-2, 84–86 cm	450.24	58.72	0.10	13.32	6.58	0.10	8.16	8.25	1.60	0.52	0.00	1.70	97.36
32R-2, 86–88 cm	461.36	71.89	0.23	13.00	3.90	0.02	0.00	2.91	3.39	1.37	0.00	1.16	96.72
34R-3, 45–47 cm	481.25	55.18	0.15	12.29	7.90	0.13	9.53	11.70	1.50	0.61	0.00	5.76	98.34
35R-1, 73–76 cm	488.73	63.60	0.20	15.13	5.84	0.04	3.31	5.59	3.07	0.53	0.00	1.75	97.28
35R-2, 122–126 cm	490.72	65.63	0.23	14.91	5.46	0.04	2.39	5.06	2.97	0.70	0.00	1.25	97.27
37R-1, 95–98 cm	508.35	57.87	0.20	15.16	7.40	0.08	6.69	7.96	2.01	0.48	0.00	2.35	97.82
37R-3, 45–49 cm	510.81	61.13	0.21	15.61	8.52	0.11	2.81	5.34	2.27	1.53	0.00	5.70	97.50
38R-3, 6–8 cm	520.12	60.82	0.22	16.43	7.23	0.09	2.16	6.89	2.11	1.06	0.00	3.03	97.00
40R-2, 54–57 cm	538.14	50.03	0.23	12.77	8.53	0.15	12.08	12.61	0.94	0.28	0.00	5.78	97.60
49R-4, 32–37 cm	623.22	60.12	0.24	15.49	7.32	0.13	3.73	7.51	2.10	0.75	0.00	2.98	97.39
51R-1, 51–55 cm	642.71	54.36	0.15	13.01	8.67	0.17	12.62	7.94	1.19	0.27	0.08	2.05	98.43
61R-5, 56–58 cm	735.06	73.70	0.24	13.37	3.32	0.05	0.00	2.54	3.41	1.13	0.00	1.88	96.94
61R-5, 81–84 cm	735.31	72.10	0.26	12.78	3.41	0.04	0.00	01.80	3.91	1.16	0.00	1.45	95.52
62R-3, 40–42 cm	741.60	55.91	0.15	12.60	8.83	0.14	13.64	5.51	2.28	0.70	0.00	4.53	99.20
63R-2, 72–74 cm	750.22	74.50	0.17	12.44	1.93	0.01	0.00	0.45	2.52	4.99	0.00	0.27	97.01
65R-1, 17–19 cm	767.57	56.18	0.36	17.62	7.62	0.08	5.60	6.73	2.13	0.50	0.00	3.34	96.82
66R-1, 88–90 cm	777.90	70.66	0.18	13.74	4.17	0.08	0.84	2.32	2.28	3.20	0.00	2.42	97.46
67R-1, 63–65 cm	787.33	54.43	0.16	12.80	7.74	0.14	13.43	6.88	1.31	0.22	0.00	2.63	97.13
69R-1, 65–67 cm	793.95	62.36	0.16	11.75	6.78	0.09	9.23	3.98	2.05	0.06	0.00	4.31	96.43

3. Production of high-Ca boninites (e.g., those found in the Troodos Massif, Cyprus, and the North Tonga Forearc) from depleted oceanic lithosphere through contact melting adjacent to rising, more fertile, upper mantle diapirs; this type should be preceded by normal island-arc lavas and should be succeeded by a rifting event, with eruption of MORB or back-arc basin lavas.

In the sense that the high-Ca boninites (Group 1) from Site 786 and from Leg 126 Site 793 are penecontemporaneous with the Oligocene rifting event that formed the Bonin Trough (Fig. 1), the hypothesis of Crawford et al. (1989) that high-Ca boninite precedes rifting events such as backarc basin formation appears to be substantiated. It is more likely, however, that the Bonin Trough formed in a forearc setting and is floored by boninite-related lavas (Shipboard Scientific Party, 1990c). Furthermore, the temporal sequence of low-Ca Type 3 followed by low-Ca Type 1 boninites proposed by Crawford et al. (1989) is not clearly demonstrated for Site 786.

A critically important comparison between the composition of the ash sequences recovered from Holes 782A, 784A, and 786A (Arculus and Bloomfield, this volume) and the Eocene through Oligocene to middle Miocene igneous lithologies recovered at Sites 782, 786, and 793 in the present-day Bonin forearc is relevant to the nature and geometric dispositon of the upper mantle sources involved. For example, it is of critical interest to determine whether the refractory, highly-depleted upper mantle sources of the boninitic sequences are isolated beneath the forearc, or persist westward beneath the active, subaerial arc. And the suggestion by Crawford et al. (1989) that high-Ca boninite may precede a rifting event is again relevant.

For example, Honza and Tamaki (1985) and other authors suggested that the following sequence of events was involved in the construction of the Bonin arc system:

1. Arc inception in the middle Eocene, now represented by the lithologies in the FBH;
2. Persistence of this locus of arc magmatism into the Oligocene;
3. Formation of the Bonin Trough in a backarc rifting event and as a forerunner to the inception and evolution of the Shikoku Basin;

Table 3 (continued).

Sample	Nb	Zr	Y	Sr	Pb	Zn	Cu	Ni	Cr	Ce	Ba
125-786A-											
6X-5, 24–27 cm	1	40	24	181	6	113	166	18	23	26	77
12X-1, 140–142 cm	2	46	6	165	14	92	40	85	320	10	36
13X-CC, 27–29 cm	2	27	6	100	13	63	52	268	613	3	23
16X-CC, 25–28 cm	1	33	9	147	3	68	37	190	506	3	6
17X-CC, 4–6 cm	1	22	11	93	10	73	160	215	471	5	8
19X-1, 0–30 cm											
19X-CC, 17–20 cm	1	21	9	64	7	71	23	522	1338	0	11
125-786B-											
1R-1, 61–64 cm	2	44	7	174	6	55	67	99	374	12	37
2R-1, 58–61 cm	2	45	2	178	7	53	72	85	345	14	39
3R-1, 94–97 cm	2	47	5	153	23	61	84	103	385	9	21
5R-2, 70–72 cm	1	34	13	147	6	63	63	170	333	0	18
6R-2, 128–130 cm	1	33	11	136	3	68	69	223	501	14	9
8R-1, 45–47 cm	1	51	16	227	9	73	68	41	8	8	17
9R-1, 10–15 cm	2	53	10	226	7	72	101	40	8	16	40
11R-1, 122–126 cm	2	39	6	170	6	71	40	159	471	16	17
12R-2, 14–16 cm	2	41	6	185	4	76	38	164	485	3	25
12R-2, 120–124 cm	2	37	7	166	6	53	74	116	425	13	37
16R-1, 137–141 cm	2	57	10	217	7	65	91	9	6	15	35
19R-1, 91–94 cm	2	48	9	214	8	72	78	33	35	13	31
21R-1, 26–29 cm	1	58	21	236	11	86	62	18	5	12	27
21R-1, 129–131 cm	2	76	12	148	36	49	68	6	0	13	52
21R-2, 72–76 cm	1	29	8	150	8	50	40	188	889	13	20
22R-3, 61–64 cm	2	76	14	162	41	51	26	1	0	10	58
24R-1, 9–12 cm	1	70	14	208	7	45	54	7	8	7	84
26R-1, 68–70 cm	2	75	12	195	16	40	22	2	0	10	73
30R-1, 29–31 cm	2	31	6	195	23	51	29	126	311	15	43
30R-1, 119–121 cm	2	42	8	178	16	51	13	127	443	10	45
31R-2, 84–86 cm	2	34	6	211	10	63	20	131	381	11	32
32R-2, 86–88 cm	1	74	12	173	43	39	20	2	0	6	77
34R-3, 45–47 cm	1	29	7	141	15	55	61	277	769	7	11
35R-1, 73–76 cm	2	56	10	213	8	48	34	26	50	0	59
35R-2, 122–126 cm	2	59	10	201	11	48	33	24	47	14	53
37R-1, 95–98 cm	2	38	9	186	13	68	20	149	393	0	34
37R-3, 45–49 cm	1	44	9	293	29	61	94	14	0	12	108
38R-3, 6–8 cm	2	49	9	229	14	62	66	12	0	13	54
40R-2, 54–57 cm	2	27	9	136	6	57	27	374	650	2	14
49R-4, 32–37 cm	1	45	11	185	10	58	89	39	93	9	46
51R-1, 51–55 cm	1	37	17	166	4	70	41	195	659	20	22
61R-5, 56–58 cm	1	77	14	121	18	45	56	3	0	13	91
61R-5, 81–84 cm	2	82	14	122	15	52	18	6	0	11	93
62R-3, 40–42 cm	2	34	8	110	7	63	60	306	1032	5	46
63R-2, 72–74 cm	2	78	13	47	51	41	63	1	0	15	585
65R-1, 17–19 cm	1	44	12	163	3	65	60	22	11	10	46
66R-1, 88–90 cm	2	74	11	101	34	96	50	9	33	19	332
67R-1, 63–65 cm	1	28	7	137	3	58	56	296	626	3	34
69R-1, 65–67 cm	2	44	8	143	0	75	177	212	748	10	39
70R-1, 68–73 cm	2	45	9	147	2	77	70	202	764	9	52

*All Fe reported as Fe_2O_3.

4. An absence of arc volcanism from the Miocene to early Pliocene, marking a quiescence during peak spreading in the Shikoku Basin;

5. A jump in the locus of the arc 100 km west of the Bonin Ridge (FBH) to the present-day Schichito Ridge and development through to the Holocene of a magmatic arc, locally reaching subaerial conditions.

The geochemistry of the ashes, although admittedly based on preliminary and sparse sampling, is clearly distinct when compared on the basis of Fe_2O_3-SiO_2 and TiO_2-SiO_2 covariation diagrams with the lithologies recovered from the FBH and the Bonin Trough (Fig. 11). These differences can only be attributed to the involvement of contrasted primary sources in the upper mantle. It appears that the relatively refractory upper mantle sources, first tapped in the middle Eocene during construction of the boninitic Bonin Ridge, were also subsequently involved in magma generation during Oligocene and Miocene rifting events. However, a different and more fertile source closer to that supplying most MORB and subaerial arc lavas was involved in the generation of the explosive magmas from which the ashes were derived. This source was most plausibly located to the west of the Bonin Ridge (FBH). In other words, an active arc culminating in subaerial explosive activity was established shortly after the construction of the boninitic basement, but some distance to the west of the present FBH. We found no evidence for the penetration of the FBH or Bonin Trough by any magma types like those of contemporaneous ashes.

A corollary is that the Bonin Trough represents a forearc rather than a backarc rift. The more fertile upper mantle source has been tapped at numerous intervals since at least the Oligocene; a regular resupply of this mantle is implicated, together with the prolonged isolation of the refractory mantle beneath the remainder of the forearc. Clearly further studies will be required to confirm or to refute this hypothesis, but understanding the implications for the geometry of the upper mantle and circulation of lithospheric vs. asthenospheric components through time will be tantalizing rewards for the effort.

Table 4. Combined on board and University of New England major-element and trace-element analyses of representative lithologies from Site 786, presented normalized to a major-element total of 100% volatile-free.

Sample	mbsf	Lab	Subunit	Chem. type	Probe interval	SiO_2	TiO_2	Al_2O_3	Fe_2O_3*	MnO	MgO	CaO	Na_2O	K_2O
125-786A-														
6X-5, 24–27	109.94	odp	1	9		54.02	0.85	16.66	12.64	0.21	4.24	9.97	1.06	0.35
12X-1, 140–142	107.1	odp	1	9	140–142	54.29	0.41	18.23	8.80	0.10	5.32	8.66	2.82	1.46
13X-CC, 27–29	115.57	odp	1	3	27–29	55.79	0.24	12.92	8.42	0.01	13.59	5.85	2.34	0.88
16X-CC, 25–28	145.19	odp	1	2		53.56	0.22	15.35	8.20	0.11	12.11	8.46	1.65	0.34
17X-CC, 4–6	154.04	odp	1	9		52.31	0.14	12.28	9.92	0.20	15.45	7.07	1.87	0.75
19X-1, 0–30	164.17	odp	1	2		53.88	0.22	15.34	8.27	0.11	11.67	8.55	1.42	0.54
19X-CC, 17–20	164.19	odp	1	9		50.27	0.28	11.32	9.49	0.17	19.93	6.09	2.05	0.43
125-786B-														
1R-1, 25–28	162.75	une	1	4		60.02	0.24	13.66	7.29	0.13	8.07	6.84	2.97	0.61
1R-1, 61–64	163.11	odp	1	4		61.86	0.21	12.75	7.23	0.11	8.03	6.27	3.06	0.52
1R-1, 75–79	163.25	une	1	4	75–79	61.63	0.20	12.82	7.31	0.12	8.08	6.17	2.97	0.65
1R-1, 89–93	163.39	une	1	4		62.48	0.21	12.99	6.97	0.11	7.26	6.21	3.17	0.52
2R-1, 58–61	170.08	odp	1	4		62.76	0.22	12.75	7.01	0.11	7.27	6.26	3.08	0.57
2R-1, 72–76	170.22	une	1	4		62.57	0.20	12.90	7.04	0.11	7.29	6.22	3.13	0.50
3R-1, 34–44	170.35	une	1	4		62.44	0.23	12.88	7.08	0.11	7.49	6.21	3.05	0.48
3R-1, 94–97	180.14	odp	1	4		60.04	0.23	13.86	7.82	0.12	9.05	5.62	2.48	0.85
4R-1, 109–111	190.09	une	1	4		62.99	0.22	13.11	6.85	0.11	6.85	6.14	3.13	0.57
5R-1, 23–25	198.83	une	1	4	23–25	59.99	0.26	15.38	7.09	0.10	5.95	7.09	3.33	0.77
5R-2, 1–6	200.1	une	1	4		61.57	0.24	14.92	6.76	0.11	6.13	6.52	3.21	0.49
5R-2, 70–72	200.8	odp	2	1		52.36	0.37	15.01	8.91	0.11	7.99	11.35	2.56	1.30
6R-2, 128–130	210.98	odp	2	1	137–138	52.86	0.36	14.51	8.80	0.17	11.22	9.58	2.27	0.26
6R-3, 17–22	211.37	une	2	1	17–22	54.01	0.33	14.84	8.58	0.17	10.21	9.42	2.19	0.21
8R-1, 43–44	228.03	une	3	6		56.82	0.29	18.46	7.76	0.12	4.34	7.95	3.59	0.63
8R-1, 45–47	228.05	odo	3	6		56.76	0.33	18.25	8.10	0.13	4.16	8.03	3.61	0.68
9R-1, 10–15	237.2	odp	3	6		59.09	0.25	17.98	7.83	0.12	4.03	7.92	2.18	0.60
9R-1, 15–17	237.25	une	3	6		56.43	0.30	18.53	7.93	0.12	4.61	8.17	3.38	0.48
9R-1, 113–118	238.23	haw	3	x	113–118									
11R-1, 103–108	257.33	une	4	2		57.58	0.20	14.12	7.94	0.14	9.94	7.09	2.58	0.39
11R-1, 122–126	257.52	odp	4	2	122–126	56.56	0.22	13.59	8.04	0.15	11.47	6.85	2.73	0.44
12R-2, 14–16	267.57	odp	4	2	14–16	55.07	0.16	13.90	8.40	0.15	11.71	7.28	2.99	0.31
12R-2, 120–124	268.63	odp	4	4	120–124	61.39	0.12	13.24	7.37	0.12	8.68	6.96	1.62	0.46
12R-2, 124–126	268.67	une	4	4		59.28	0.19	13.72	7.75	0.13	8.82	7.08	2.56	0.44
13R-1, 34–36	276.04	haw	4	4	34–36									
13R-2, 134–138	278.47	une	4	4		61.05	0.19	13.84	6.87	0.11	7.63	6.84	2.93	0.51
15R-1, 0–1	295.	haw	5	cum	0–1									
15R-2, 3–8	296.53	une	5	6	3–8	61.17	0.32	17.13	7.66	0.11	3.02	6.21	3.52	0.77
16R-1, 135–138	305.95	une	5	7		64.68	0.30	15.76	6.78	0.10	2.03	5.77	3.86	0.69
16R-1, 137–141	305.97	odp	5	7		64.94	0.34	15.68	7.08	0.09	1.69	5.77	3.69	0.76
16R-2, 12–17	306.22	une	5	6		61.69	0.32	16.84	7.66	0.12	2.88	6.07	3.63	0.76
17R-1, 67–69	314.97	une	5	6	67–69	60.27	0.33	17.72	7.83	0.09	2.03	6.56	4.47	0.50
17R-1, 81–83	315.11	haw	5	6	81–83									
19R-1, 10–17	333.7	une	6	6		58.80	0.29	17.35	7.70	0.13	4.31	7.57	3.16	0.65
19R-1, 91–94	334.51	odp	6	6	91–94	60.12	0.30	16.81	7.75	0.12	3.69	7.38	3.13	0.73
20R-1, 43–46	343.73	une	7	2		54.82	0.23	12.78	8.49	0.19	12.43	8.52	2.16	0.37
20R-1, 72–74	344.02	une	7	2		55.53	0.23	13.15	8.66	0.19	11.25	8.46	2.16	0.36
20R-1, 124–128	344.54	une	6	6		61.82	0.30	17.04	7.22	0.10	2.51	6.41	3.93	0.50
21R-1, 26–29	353.26	odp	6	6		59.86	0.35	17.85	8.11	0.11	1.95	6.91	3.90	0.90
21R-1, 26–30	353.26	une	6	6		60.57	0.32	17.75	7.27	0.07	1.75	6.71	4.33	0.87
21R-1, 129–131	354.29	odp	8	8	129–132	72.99	0.29	13.77	3.81	0.08	0.34	2.51	3.99	2.24
21R-2, 28–32	354.7	une	8	8	28–32	71.12	0.26	14.23	3.92	0.09	0.92	2.76	4.19	2.46
21R-2, 72–76	355.2	odp	9	1	72–76	54.65	0.24	12.74	8.79	0.15	6.24	14.39	2.38	0.42
21R-2, 103–107	355.46	une	9	1		55.40	0.22	12.81	8.43	0.16	10.74	9.37	2.56	0.26
22R-3, 61–64	370.	odp	10	8		73.43	0.29	13.47	3.65	0.07	0.12	2.18	4.15	2.64
24R-1, 9–12	381.99	odp	11	7		67.91	0.35	15.24	5.32	0.07	0.91	4.58	4.74	0.84
24R-1, 41–45	383.31	une	11	7		67.85	0.32	15.04	5.15	0.08	1.39	4.36	4.74	0.98
24R-2, 5–9	383.45	une	11	7	5–9	67.39	0.30	15.17	5.38	0.08	1.54	4.58	4.45	1.05
25R-1, 64–72	392.14	une	11	7		66.93	0.32	15.51	5.13	0.08	1.29	4.58	4.88	1.09
26R-1, 68–70	401.88	odp	11	7		68.93	0.33	15.18	4.93	0.06	0.57	3.96	4.81	1.19
27R-1, 31–35	411.11	une	11	7		68.37	0.31	14.87	5.11	0.07	1.48	4.17	4.59	0.98
28R-1, 15–18	420.55	une	13	4		59.59	0.16	13.19	7.23	0.13	8.97	7.57	2.70	0.44
29R-1, 63–66	430.73	une	14	1		52.84	0.21	12.02	8.17	0.20	10.88	13.13	2.17	0.19
30R-1, 7–9	439.77	une*	13	4		59.00	0.24	13.87	6.78	0.11	8.11	8.15	3.08	0.57
30R-1, 29–31	439.99	odp	13	4	29–31	58.92	0.15	12.83	7.34	0.09	6.86	10.34	2.56	0.91
30R-1, 119–121	440.89	odp	13	4		61.89	0.15	13.69	6.76	0.10	5.95	8.54	2.19	0.74
30R-2, 39–45	441.59	une	13	4		60.70	0.22	14.07	6.72	0.12	5.05	8.68	3.56	0.85
30R-2, 136–139	442.63	une*	15	1		53.50	0.40	14.95	8.65	0.17	10.26	9.36	2.39	0.26
31R-2, 84–86	450.24	odp	13	4	86–87	59.54	0.16	13.50	6.67	0.10	8.27	8.37	5.87	0.53
31R-1, 102–109	450.42	une	13	4		61.45	0.22	14.22	6.40	0.08	6.23	7.26	3.48	0.62
32R-2, 86–88	461.36	odp	16	8		73.36	0.24	13.27	3.98	0.02	0.00	2.97	4.66	1.39
34R-3, 45–47	481.25	odp	19	1		55.16	0.22	12.29	7.89	0.13	9.52	11.69	2.52	0.61
34R-4, 14–20	482.84	une	19	1	14–21	56.15	0.21	12.15	8.29	0.13	9.59	10.20	2.65	0.62
35R-1, 73–76	488.73	odp	20	7		64.92	0.28	15.44	5.96	0.04	3.38	5.70	3.72	0.54
35R-1, 127–130	489.29	une*	20	9		60.56	0.32	13.68	5.27	0.08	2.21	12.92	3.67	1.16
35R-2, 1–7	489.51	une	20	7		65.78	0.29	15.31	5.53	0.05	2.86	5.01	4.57	0.52
35R-2, 122–126	490.72	odp	20	7	122–126	66.72	0.28	15.16	5.55	0.04	2.43	5.15	3.93	0.71
36R-1, 52–59	498.22	une	20	8		71.29	0.28	13.59	4.03	0.03	1.54	3.29	4.79	1.06
37R-1, 95–98	508.35	odp	21	4	95–98	58.61	0.26	15.35	7.50	0.08	6.77	8.06	2.86	0.49
37R-3, 13–15	510.45	une	21	2		56.85	0.26	14.58	8.20	0.09	8.44	8.25	2.82	0.40

Table 4 (continued).

Sample	P_2O_5	S	LOI	Nb	Zr	Y	Sr	Rb	Th	Pb	U	Ga	Zn	Cu	Ni	Cr	La	Ce	Nd	Ba	V	Sc
125-786A																						
6X-5, 24–27	0.00	0.00	0.84	1	40	24	181	6					113	166	18	23		26		77	428	
12X-1, 140–142	0.02	0.00	2.92	2	46	6	165	14					92	40	85	320		10		36	356	
13X-CC, 27–29	0.02	0.00	5.79	2	27	6	100	13					63	52	268	613		3		23	143	
16X-CC, 25–28	0.00	0.00	2.41	1	33	9	147	3					68	37	190	506		3		6	226	
17X-CC, 4–6	0.00	0.00	6.16	1	22	11	93	10					73	160	215	471		5		8	194	
19X-1, 0–30	0.00	0.00	4.66																			
19X-CC, 17–20	0.02	0.00	5.21	1	21	9	64	7					71	23	522	1338		0		11	195	
125-786B-																						
1R-1, 25–28	0.17	0.01	4.01																			
1R-1, 61–64	0.02	0.00	2.19	2	44	7	174	6					55	67	99	374		12		37	177	
1R-1, 75–79	0.03	0.01	2.81																			
1R-1, 89–93	0.03	0.04	3.35	1	40	7	167	8	0	2	1	9	58	62	96	471	4	1	0	54	153	24
2R-1, 58–61	0.04	0.00	2.05	2	45	2	178	7					53	72	85	345		14		39	185	
2R-1, 72–76	0.03	0.01	3.11	1	42	6	165	7	0	1	1	8	58	68	91	471	3	6	0	48	152	27
3R-1, 34–44	0.03	0.00	2.95	0	41	6	168	8	2	3	1	9	59	65	91	456	5	0	0	63	150	30
3R-1, 94–97	0.01	0.00	3.78	2	47	5	153	23					61	84	103	385		9		21	100	
4R-1, 109–111	0.03	0.00	1.93	0	44	6	170	7	2	2	2	11	60	74	85	405	6	6	2	67	163	25
5R-1, 23–25	0.02	0.01	4.40																3			
5R-2, 1–6	0.03	0.01	3.68	1	49	9	198	7	0	2	0	12	64	55	64	238	4	8	2	58	157	22
5R-2, 70–72	0.10	0.00	3.40	1	34	13	147	6					63	63	170	333		0		18	237	
6R-2, 128–130	0.05	0.00	1.90	1	33	11	136	3					68	69	223	501		14		9	232	
6R-3, 17–22	0.04	0.00	3.84	0	31	10	129	3	0	0	2	11	67	54	202	564	3	0	0	11	229	32
8R-1, 43–44	0.03	0.01	5.01																			
8R-1, 45–47	0.05	0.00	2.71	1	51	16	227	9					73	68	41	8		8		17	236	
9R-1, 10–15	0.00	0.00	1.97	2	53	10	226	7					72	101	40	8		16		40	239	
9R-1, 15–17	0.03	0.01	4.56																			
9R-1, 113–118																						
11R-1, 103–108	0.01	0.01	4.72	1	39	5	174	5	0	0	0	12	71	41	149	580	5	10	1	50	153	32
11R-1, 122–126	0.01	0.00	2.80	39	6	170	6					71	40	159	471		16		17	174		
12R-2, 14–16	0.01	0.00	2.16	2	2	41	6	185	4					76	38	164	485		3		25	153
12R-2, 120–124	0.03	0.00	1.53	2	37	7	166	6					53	74	116	425		13		37	187	
12R-2, 124–126	0.02	0.01	3.17	0	35	6	157	6	3	3	2	9	65	58	127	564	5	0	0	42	184	40
13R-1, 34–36																						
13R-2, 134–138	0.03	0.00	2.37	1	37	6	178	7	0	1	3	9	57	65	116	473	5	0	0	45	169	26
15R-1, 0–1																						
15R-2, 3–8	0.04	0.06	6.99	1	56	12	217	7	2	1	3	16	78	75	17	8	4	9	5	42	203	20
16R-1, 135–138	0.04	0.00	3.43																			
16R-1, 137–141	0.04	0.00	2.48	2	57	10	217	7					65	91	9	6		15		35	219	
16R-2, 12–17	0.03	0.01	4.84	1	57	9	217	9	1	0	0	14	80	80	17	15	7	1	0	39	205	28
17R-1, 67–69	0.17	0.02	2.88	1	61	35	248	6	3	4	2	17	76	69	13	10	11	16	10	77	219	23
17R-1, 81–83																						
19R-1, 10–17	0.03	0.01	4.35	0	49	11	210	6	1	3	1	13	79	82	38	67	2	2	0	20	202	27
19R-1, 91–94	0.04	0.00	2.34	2	48	9	214	8					72	78	33	35		13		31	226	
20R-1, 43–46	0.01	0.01	5.08																			
20R-1, 72–74	0.00	0.01	5.77																			
20R-1, 124–128	0.07	0.08	4.76	1	57	21	217	6	2	3	3	13	72	83	22	12	9	7	5	61	197	29
21R-1, 26–29	0.15	0.00	2.91	1	58	21	236	11					86	62	18	5		12		27	21	
21R-1, 26–30	0.33	0.02	5.21	0	56	28	233	13	3	4	1	16	59	78	16	17	10	19	4	54	190	21
21R-1, 129–131	0.07	0.00	6.50	2	76	12	148	36					49	68	6	0		13		52	24	
21R-2, 28–32	0.07	0.00	7.59	1	79	12	128	30	0	2	1	10	54	61	13	3	7	9	4	68	19	15
21R-2, 72–76	0.08	0.00	5.75	1	29	8	150	8					50	40	188	889		13		20	185	
21R-2, 103–107	0.04	0.00	6.02	1	28	7	133	5	2	4	2	10	71	63	275	1004	3	3	0	25	165	31
22R-3, 61–64	0.11	0.00	7.97	2	76	14	162	41					51	26	1	0		10		58	54	
24R-1, 9–12	0.11	0.00	0.44	1	70	14	208	7					45	54	7	8		7		84	185	
24R-1, 41–45	0.11	0.00	1.10	1	71	15	199	13	4	3	0	15	49	49	7	14	7	6	2	80	153	19
24R-2, 5–9	0.06	0.00	2.62	1	67	10	189	10	3	5	1	9	55	97	8	15	4	6	1	69	183	13
25R-1, 64–72	0.20	0.00	0.95	0	72	12	207	12	1	2	1	14	48	40	6	7	6	9	1	68	163	13
26R-1, 68–70	0.09	0.00	0.31	2	75	12	195	16					40	22	2	0		10		73	119	
27R-1, 31–35	0.06	0.00	5.45																			
28R-1, 15–18	0.02	0.00	2.62	0	33	5	192	6	3	2	2	8	58	62	134	491	4	4	0	36	153	31
29R-1, 63–66	0.20	0.00	7.08	25	5	138	5	1	1	1	8	76	34	245	956	6	4	0	53	160	36	
30R-1, 7–9	0.08	0.01	3.39	0	1	33	5	207	9	1	2	1	11	65	29	136	524	2	7	4	56	166
30R-1, 29–31	0.06	0.00	4.23	2	31	6	195	23					51	29	126	311		15		43	132	
30R-1, 119–121	0.00	0.00	3.43	2	42	8	178	16					51	13	127	443		10		45	142	
30R-2, 39–45	0.04	0.00	4.82	1	29	5	129	15	1	1	1	8	48	13	92	513	4	4	0	64	141	33
30R-2, 136–139	0.06	0.01	4.65	1	32	10	130	4	3	2	1	13	65	57	188	552	4	5	0	3	231	35
31R-2, 84–86	0.04	0.00	1.67	2	34	6	211	10					63	20	131	381		11		32	184	
31R-1, 102–109	0.04	0.00	3.72	0	42	7	174	10	0	0	2	11	57	29	129	585	6	4	0	82	160	26
32R-2, 86–88	0.11	0.00	1.15	1	74	12	173	43					39	20	2	0		6		77	46	
34R-3, 45–47	0.03	0.00	5.44	1	29	7	141	15					55	61	277	769		7		11	160	
34R-4, 14–20	0.02	0.00	6.47	1	26	6	128	15	1	1	3	7	48	47	246	930	4	2	0	38	145	35
35R-1, 73–76	0.08	0.00	1.72	2	56	10	213	8					48	34	26	50		0		59	152	
35R-1, 127–130	0.09	0.04	8.70	1	52	9	173	31	4	4	0	12	55	22	17	53	4	9	6	55	98	26
35R-2, 1–7	0.06	0.01	4.09	1	62	10	201	8	1	0	3	12	64	58	19	43	5	5	1	80	121	16
35R-2, 122–126	0.08	0.00	1.23	2	59	10	201	11					48	33	24	47		14		53	134	
36R-1, 52–59	0.09	0.01	2.60	1	70	13	171	22	3	1	1	12	51	21	5	14	3	6	1	80	56	12
37R-1, 95–98	0.06	0.00	2.29	2	38	9	186	13					68	20	149	393		0		34	185	
37R-3, 13–15	0.04	0.05	4.41	0	30	9	153	14	2	5	1	12	69	21	19.	724	3	0	0	38	196	31

Table 4 (continued).

Sample	mbsf	Lab	Subunit	Chem. type	Probe interval	SiO_2	TiO_2	Al_2O_3	Fe_2O_3	MnO	MgO	CaO	Na_2O	K_2O
125-786B-														
37R-3, 31–35	510.63	haw	21	2	31–35									
37R-3, 45–49	510.81	odp	22	6		62.27	0.29	15.91	8.68	0.11	2.86	5.45	2.88	1.56
38R-1, 6–8	517.16	odp	22	6		62.17	0.30	16.79	7.39	0.09	2.20	7.04	2.96	1.09
38R-1, 57–60	517.67	haw	22	6	57–60									
38R-1, 76–83	517.86	une	22	6		61.17	0.26	16.34	8.11	0.11	3.36	5.63	3.48	1.16
39R-1, 47–53	527.27	une	22	6		62.00	0.28	17.16	6.55	0.07	2.44	7.11	3.85	0.44
39R-2, 119–123	529.49	une	22	6		62.73	0.35	15.14	8.01	0.11	2.73	6.47	3.58	0.81
40R-2, 54–57	538.14	odp	23	1	54–56	50.68	0.30	12.94	8.64	0.15	12.23	12.77	2.03	0.28
40R-2, 83–90	538.41	une	23	1		52.04	0.29	13.30	8.74	0.16	10.20	12.70	2.23	0.32
42R-2, 15–21	558.25	une	24	4		60.13	0.24	15.29	6.03	0.07	6.57	7.13	3.59	0.86
42R-4, 46–54	560.51	une	24	4		61.58	0.22	14.38	6.52	0.08	6.45	6.69	3.42	0.61
43R-2, 43–52	566.73	une	24	4	43–52	59.94	0.22	14.61	6.43	0.10	6.00	8.40	3.61	0.66
43R-2, 100–105	567.3	une	24	4		60.57	0.23	14.47	6.68	0.10	6.37	7.28	3.45	0.77
44R-1, 38–45	574.98	une	25	2		53.73	0.31	13.44	9.20	0.20	12.16	8.16	2.42	0.36
44R-1, 102–109	575.62	une	25	2		53.47	0.30	13.03	9.11	0.22	13.19	8.01	2.30	0.35
45R-1, 41–49	584.71	une	24	4		61.59	0.33	14.90	7.36	0.11	4.82	6.74	3.45	0.67
46R-1, 39–43	594.29	une*	24	4		59.84	0.41	15.32	7.52	0.14	5.49	6.97	3.48	0.77
46R-1, 119–125	595.09	une*	24	4		60.36	0.41	15.22	7.51	0.13	5.32	6.95	3.10	0.89
46R-2, 54–58	595.94	une*	24	4		59.70	0.38	15.43	7.66	0.14	6.26	6.69	3.09	0.60
47R-1, 18–22	603.68	une*	24	4		59.12	0.33	15.37	7.72	0.16	6.04	7.48	3.09	0.64
47R-1, 112–116	604.62	une*	24	4		56.72	0.34	16.15	8.36	0.16	7.28	6.86	3.06	0.98
48R-1, 48–53	613.68	une*	24	4		51.01	0.41	17.83	10.27	0.10	4.67	9.24	3.82	1.04
49R-2, 99–103	624.95	une*	24	4		57.35	0.41	15.73	8.41	0.19	7.09	6.61	3.20	0.95
49R-4, 32–37	627.	odp	24	6	32–37	61.20	0.35	15.77	7.45	0.14	3.80	7.65	2.96	0.77
50R-1, 137–141	633.87	une*	24	4		59.75	0.32	14.50	7.98	0.14	7.26	6.44	2.97	0.58
50R-2, 45–48	635.86	une*	24	4		59.82	0.32	13.17	7.51	0.15	9.06	6.43	2.97	0.52
51R-1, 49–56	642.69	une	26	2		56.12	0.21	13.17	8.41	0.16	11.20	7.81	2.38	0.36
51R-1, 51–55	642.71	odp	26	2	51–55	54.24	0.25	12.98	8.65	0.17	12.59	7.92	2.78	0.26
51R-2, 5–9	643.75	une*	26	2		55.07	0.30	13.25	8.75	0.17	11.63	7.88	2.43	0.28
52R-1, 112–116	653.02	une*	26	2–4		58.21	0.27	13.25	8.93	0.17	10.44	5.55	2.38	0.78
53R-1, 66–72	662.26	une*	26	2–4		58.16	0.27	12.38	8.63	0.33	9.03	8.13	2.48	0.54
53R-1, 82–85	662.42	une*	26	4		58.97	0.28	13.02	7.67	0.24	8.80	7.97	2.47	0.52
53R-2, 12–14	663.22	haw	26	4	12–14									
54R-1, 50–54	671.7	une*	26	2		58.14	0.28	12.42	7.91	0.16	10.42	7.83	2.37	0.44
54R-2, 26–30	672.96	une*	26	2–4		59.35	0.26	12.82	8.00	0.15	10.20	6.28	2.40	0.50
54R-2, 84–88	673.54	une*	26	2		57.87	0.27	12.89	8.60	0.16	10.09	7.08	2.38	0.61
54R-2, 144–147	674.14	une*	26	2–4		59.69	0.27	12.99	7.89	0.14	9.71	6.44	2.36	0.46
54R-3, 60–65	674.8	une*	26	2–4		59.66	0.29	12.95	8.01	0.15	10.08	6.28	2.04	0.49
54R-4, 75–79	676.45	une*	26	2–4		59.60	0.28	13.19	7.81	0.14	9.86	6.33	2.27	0.48
54R-5, 8–15	676.98	une*	26	2–4		59.74	0.29	12.96	8.05	0.14	9.65	6.45	2.23	0.45
55R-1, 15–18	680.95	haw	26	4	15–18									
55R-1, 87–91	681.67	une*	26	4		59.48	0.34	12.81	8.31	0.27	7.97	7.69	2.44	0.62
55R-2, 11–16	682.31	une*	26	4		60.20	0.29	13.15	7.86	0.16	8.25	7.10	2.38	0.57
55R-3, 44–49	684.09	une*	26	3		59.34	0.32	11.91	7.97	0.18	12.70	4.91	2.18	0.43
56R-2, 51–56	692.11	une	26	3		57.11	0.22	12.13	8.10	0.12	13.14	5.02	2.86	1.28
57R-2, 124–128	702.46	une*	27	9		54.03	0.24	11.85	10.15	0.21	14.95	4.53	3.06	0.92
57R-4, 69–77	704.7	une	27	3		56.28	0.21	12.19	8.27	0.15	13.64	5.48	3.23	0.54
58R-1, 116–120	710.56	une*	27	3		58.36	0.25	11.36	8.21	0.13	12.46	5.54	3.55	0.08
58R-3, 62–69	712.83	une	27	5		62.08	0.18	10.81	6.99	0.12	10.86	5.02	3.81	0.11
59R-3, 84–91	717.92	une	27	3	84–91	56.62	0.19	11.33	8.46	0.14	14.09	5.35	3.72	0.06
60R-3, 102–108	722.77	une	27	5		61.12	0.18	10.73	7.16	0.13	11.54	5.17	3.81	0.15
61R-4, 96–102	733.96	une	28	8		70.88	0.32	13.38	4.63	0.07	0.56	3.52	4.84	1.72
61R-5, 56–58	735.06	odp	28	8		73.61	0.33	13.36	3.32	0.05	0.00	2.54	5.66	1.13
61R-5, 81–84	735.31	odp	28	8		73.51	0.20	13.03	3.48	0.04	0.00	1.83	6.55	1.18
62R-1, 114–120	739.54	une	27	5		61.94	0.19	10.74	7.19	0.09	12.13	3.86	3.32	0.44
62R-3, 40–42	741.6	odp	27	3	40–42	55.56	0.15	12.52	8.77	0.14	13.55	5.48	3.11	0.70
63R-2, 72–74	750.22	odp	29	8		74.95	0.27	12.52	1.94	0.01	0.00	0.45	4.85	5.02
63R-2, 86–91	750.36	une	29	8		76.33	0.23	12.19	2.49	0.04	0.29	1.41	3.33	3.56
64R-2, 93–105	760.03	une	29	8		73.08	0.23	12.60	3.81	0.05	0.98	1.72	3.39	4.09
65R-1, 17–19	767.57	odp	30	6		57.44	0.41	18.01	7.79	0.08	5.72	6.88	3.13	0.51
65R-1, 21–25	767.61	une	30	6		57.28	0.42	18.05	7.56	0.09	5.72	6.78	3.54	0.51
65R-2, 5–12	768.95	une	29	8		72.85	0.24	13.21	3.72	0.05	1.28	1.11	3.67	3.77
66R-1, 26–33	777.36	une	29	8		71.92	0.25	13.47	3.98	0.07	1.27	2.23	3.70	2.97
66R-1, 88–90	777.9	odp	29	8		71.42	0.26	13.89	4.22	0.08	0.85	2.34	3.70	3.23
66R-3, 18–24	780.23	une	29	8		73.49	0.23	13.05	3.32	0.06	0.96	0.85	3.24	4.70
67R-1, 33–41	787.03	une	29	8		76.03	0.23	12.51	2.60	0.03	0.40	1.19	4.25	2.71
67R-1, 63–65	787.33	odp	32	2	62–63	55.34	0.22	13.01	7.87	0.15	13.66	7.00	2.56	0.22
69R-1, 65–67	797.95	odp	33	5		63.98	0.22	12.06	6.96	0.09	9.47	4.08	3.10	0.06
69R-1, 68–77	797.98	une	33	5		64.60	0.23	12.46	6.05	0.08	8.29	3.30	4.10	0.14
69R-4, 105–113	802.36	une	33	5		62.52	0.23	12.40	6.44	0.13	8.50	4.94	3.93	0.10
69R-5, 60–64	803.07	une	33	5		63.64	0.21	11.75	7.11	0.09	8.24	3.93	3.38	0.07
69R-7, 34–42	805.68	une	33	5		62.30	0.22	12.39	6.90	0.13	9.10	4.42	4.23	0.16
70R-1, 68–73	807.58	odp	33	5	68–72	63.62	0.23	12.44	6.65	0.14	8.06	5.39	3.28	0.22
70R-1, 92–96	807.82	une*	33	5		62.39	0.26	11.77	6.82	0.19	8.73	6.04	3.43	0.20
70R-2, 5–11	808.45	une	33	5		62.33	0.22	12.16	6.73	0.17	8.20	6.40	3.42	0.28
70R-4, 11–17	811.32	une	33	3		58.94	0.26	14.20	7.98	0.10	10.52	3.05	2.80	0.41
71R-4, 7–12	819.99	une	33	5		61.52	0.26	15.23	6.27	0.09	8.21	4.45	2.96	0.42
71R-4, 74–80	820.66	une	33	5		61.55	0.24	14.82	6.36	0.06	7.22	5.44	3.39	0.11
71R-4, 141–146	812.33	une	33	5	141–146	60.39	0.24	14.27	7.23	0.06	7.09	5.66	3.32	0.09
72R-1, 3–7	823.63	une*	34	4		60.81	0.32	15.23	7.10	0.05	8.25	1.49	3.20	0.92
72R-1, 91–96	824.51	haw	33	5	91–96									

Table 4 (continued).

Sample	P_2O_5	S	LOI	Nb	Zr	Y	Sr	Rb	Th	Pb	U	Ga	Zn	Cu	Ni	Cr	La	Ce	Nd	Ba	V	Sc
125-786B-																						
37R-3, 31–35																						
37R-3, 45–49	0.07	0.00	5.39	1	44	9	293	29					61	94	14	0		12		108	224	
38R-1, 6–8	0.04	0.00	2.94	2	49	9	229	14					62	66	12	0		13		54	259	
38R-1, 57–60																						
38R-1, 76–83	0.02	0.35	8.74	1	43	6	261	21	3	2	2	13	58	84	53	10	2	7	1	58	196	16
39R-1, 47–53	0.09	0.00	2.87	0	47	11	236	5	1	0	3	14	112	32	14	11	6	4	2	53	238	24
39R-2, 119–123	0.04	0.02	3.51	1	48	11	173	16	2	1	1	13	67	108	15	11	4	8	3	54	270	26
40R-2, 54–57	0.04	0.00	5.46	2	27	9	136	6					57	27	374	650		2		14	193	
40R-2, 83–90	0.02	0.00	8.00	0	23	8	131	7	1	1	2	10	59	34	349	961	2	3	0	25	187	38
42R-2, 15–21	0.06	0.03	4.50	0	42	8	191	9	1	3	2	14	52	39	88	387	8	4	0	66	171	27
42R-4, 46–54	0.04	0.02	4.30	1	40	6	179	8	1	1	0	11	52	44	90	356	3	4	0	64	166	25
43R-2, 43–52	0.03	0.00	6.11	1	31	6	140	7	1	1	1	9	36	10	68	272	3	1	0	46	117	18
43R-2, 100–105	0.04	0.04	5.32	0	41	7	183	7	1	0	2	11	55	10	94	382	3	0	0	55	161	30
44R-1, 38–45	0.03	-0.01	6.15	0	26	8	117	7	1	0	1	11	62	44	315	804	0	0	0	23	190	28
44R-1, 102–109	0.02	-0.01	7.30	0	26	7	107	8	1	0	1	9	67	157	367	915	4	4	3	38	193	26
45R-1, 41–49	0.04	0.00	2.52	1	45	9	172	10	0	0	2	13	62	100	56	193	4	4	0	68	228	24
46R-1, 39–43	0.06	0.01	4.52	1	46	13	177	9	2	3	0	13	62	76	61	178	6	6	5	46	264	27
46R-1, 119–125	0.10	0.01	2.91	0	47	10	178	10	2	3	0	13	61	89	60	185	8	4	4	52	242	23
46R-2, 54–58	0.04	0.01	6.70	1	45	10	170	9	3	6	0	13	66	73	65	183	5	11	4	24	236	28
47R-1, 18–22	0.04	0.01	4.50	0	41	8	173	8	2	4	0	14	65	68	70	247	7	7	4	65	215	26
47R-1, 112–116	0.02	0.02	11.20	1	41	5	156	15	3	6	2	13	60	93	72	230	9	3	3	27	118	29
48R-1, 48–53	1.59	0.04	6.90	0	47	95	233	37	4	4	2	25	104	86	47	166	32	58	20	48	269	33
49R-2, 99–103	0.06	0.02	10.00	1	42	8	188	15	3	3	0	13	64	88	90	189	8	5	2	41	195	23
49R-4, 32–37	0.04	0.00	2.89	1	45	11	185	10					58	89	39	93		9		46	245	
50R-1, 137–141	0.04	0.02	6.76	0	40	7	150	9	1	2	0	12	60	112	108	395	3	1	1	27	171	23
50R-2, 45–48	0.05	0.01	3.74	0	38	6	155	9	3	4	1	11	60	70	184	763	4	1	1	62	169	25
51R-1, 49–56	0.16	0.03	3.91	1	33	17	151	5	0	0	0	11	67	44	196	921	7	14	6	56	212	31
51R-1, 51–55	0.25	0.00	2.01	1	37	17	166	4					70	41	195	659		20		22	228	
51R-2, 5–9	0.19	0.03	4.77	0	34	18	152	3	5	6	1	11	69	56	197	887	7	13	6	35	211	33
52R-1, 112–116	0.02	0.01	13.00	1	33	2	108	14	3	16	2	11	87	92	172	687	5	4	1	42	92	27
53R-1, 66–72	0.04	0.01	8.92	0	31	6	131	12	2	4	1	12	57	72	252	697	3	1	4	59	146	26
53R-1, 82–85	0.06	0.01	4.35	1	34	7	146	8	4	5	2	13	60	57	163	799	3	5	4	38	186	32
53R-2, 12–14																						
54R-1, 50–54	0.03	0.01	8.85	1	32	5	153	8	4	2	1	10	56	53	217	767	4	9	2	59	150	29
54R-2, 26–30	0.04	0.02	9.15	1	33	6	123	8	3	5	1	11	58	55	163	799	2	5	0	41	160	30
54R-2, 84–88	0.04	0.02	4.85	1	34	8	141	9	4	4	2	11	62	46	185	840	4	11	4	43	179	33
54R-2, 144–147	0.04	0.01	7.73	0	33	4	125	7	1	4	2	9	60	55	151	848	1	7	4	37	179	29
54R-3, 60–65	0.04	0.01	7.35	0	34	6	127	9	5	5	1	11	62	58	160	821	2	6	2	74	170	26
54R-4, 75–79	0.04	0.01	7.81	0	36	6	137	9	5	5	2	10	59	47	154	667	4	6	2	37	176	31
54R-5, 8–15	0.04	0.01	6.81	1	34	6	134	10	3	3	1	11	60	114	163	722	5	5	2	43	158	26
55R-1, 15–18																						
55R-1, 87–91	0.05	0.02	5.31	1	34	6	148	11	2	3	0	11	58	74	173	694	2	11	2	172	180	31
55R-2, 11–16	0.04	0.01	6.92	2	36	5	144	10	5	4	0	11	59	47	161	674	3	9	2	35	179	25
55R-3, 44–49	0.05	0.01	10.90	0	30	6	96	8	4	4	2	9	57	75	217	949	7	8	3	33	158	30
56R-2, 51–56	0.01	0.00	11.00	1	30	4	119	15	4	4	2	11	55	33	197	949	5	0	0	69	144	27
57R-2, 124–128	0.06	0.01	12.41	1	29	7	107	12	3	4	0	11	72	18	341	1014	7	7	0	14	135	27
57R-4, 69–77	0.01	0.00	10.50	0	30	4	106	9	1	1	1	9	61	18	281	1200	3	5	0	27	134	29
58R-1, 116–120	0.04	0.02	7.12	0	29	7	91	1	4	6	1	12	56	26	281	1065	1	3	4	29	186	26
58R-3, 62–69	0.03	0.00	7.25	0	25	6	83	3	0	1	2	8	50	50	247	1017	3	1	0	20	192	27
59R-3, 84–91	0.03	0.00	7.46	1	29	6	91	0	1	1	2	9	61	29	289	1128	1	0	0	30	144	28
60R-3, 102–108	0.02	0.00	6.55	0	26	5	80	2	1	1	0	11	53	43	271	999	5	0	0	21	203	25
61R-4, 96–102	0.08	0.00	2.93	0	81	15	123	28	2	3	2	13	57	32	4	8	6	9	5	175	38	12
61R-5, 56–58	0.10	0.00	1.84	1	77	14	121	18					45	56	3	0		13		91	35	
61R-5, 81–84	0.11	0.00	1.43	2	82	14	122	15					52	18	6	0		11		93	41	
62R-1, 114–120	0.02	0.08	9.58	1	28	7	88	6	2	2	0	9	58	145	269	977	4	2	1	55	121	27
62R-3, 40–42	0.03	0.00	4.33	2	34	8	110	7					63	60	306	1032		5		46	166	
63R-2, 72–74	0.08	0.00	0.27	2	78	13	47	51					41	63	1	0		15		585	22	
63R-2, 86–91	0.05	0.07	0.93	1	71	10	93	32	1	1	1	7	86	31	4	14	4	15	2	679	27	13
64R-2, 93–105	0.05	0.01	1.68	1	72	12	77	37	3	3	2	9	67	30	11	22	3	11	3	756	33	13
65R-1, 17–19	0.06	0.00	3.23	1	44	12	163	3					65	60	22	11		10		46	267	
65R-1, 21–25	0.05	0.00	4.95	1	44	10	160	5	3	2	2	15	75	67	21	18	4	5	0	56	241	29
65R-2, 5–12	0.06	0.04	1.48	1	75	11	91	34	1	0	1	10	63	76	7	18	5	10	6	673	31	10
66R-1, 26–33	0.06	0.07	2.51	0	75	10	108	28	2	4	1	11	92	54	5	15	4	11	5	325	29	16
66R-1, 88–90	0.08	0.00	2.36	2	74	11	101	34					96	50	9	33		19		332	31	
66R-3, 18–24	0.06	0.02	1.34	0	73	9	76	44	0	0	2	10	77	53	4	17	5	13	5	708	32	13
67R-1, 33–41	0.05	0.00	0.69	1	77	12	102	24	1	1	1	8	105	38	3	11	4	7	2	430	22	14
67R-1, 63–65	0.04	0.00	2.56	1	28	7	137	3					58	56	296	626		3		34	202	
69R-1, 65–67	0.04	0.00	4.31	2	44	8	143	0					75	177	212	748		10		39	156	
69R-1, 68–77	0.04	0.71	7.89	0	46	8	123	2	0	5	2	11	110	65	159	676	7	6	2	58	121	21
69R-4, 105–113	0.04	0.77	8.98	0	43	7	126	2	0	5	1	11	60	68	177	728	5	3	2	43	123	20
69R-5, 60–64	0.03	1.55	7.90	0	40	7	130	1	0	11	2	9	70	199	216	787	3	5	2	55	124	27
69R-7, 34–42	0.03	0.11	9.81	1	42	7	114	1	3	1	0	10	83	90	195	765	5	3	0	57	123	28
70R-1, 68–73	0.05	0.00	4.66	2	45	9	147	2					77	70	202	764		9		52	148	
70R-1, 92–96	0.06	0.13	10.16	1	42	8	122	1	3	6	0	11	88	75	196	761	3	7	1	73	118	23
70R-2, 5–11	0.03	0.06	9.32	0	42	7	133	3	1	1	3	9	65	66	191	786	7	8	2	45	122	24
70R-4, 11–17	0.03	1.70	8.12	0	34	6	104	3	0	2	2	11	65	80	212	811	2	3	0	54	205	29
71R-4, 7–12	0.03	0.57	6.15	1	40	7	136	3	0	2	1	13	107	61	120	510	4	4	0	58	186	27
71R-4, 74–80	0.03	0.77	6.97	1	38	7	164	1	2	4	2	11	139	72	109	506	5	0	0	26	193	26
71R-4, 141–146	0.03	1.63	6.97	0	38	5	162	0	0	6	3	10	101	304	180	535	4	3	1	25	194	32
72R-1, 3–7	0.05	2.57	7.43	0	37	7	142	8	1	3	1	10	39	22	183	805	4	4	3	66	182	32
72R-1, 91–96																						

All Fe reported as Fe_2O_3. Une refers to a second batch of analyses at the University of New England.

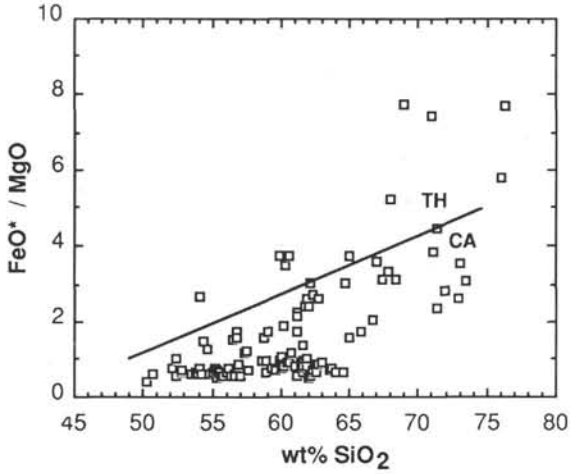

Figure 5. Variation of FeO* (total Fe as FeO)/MgO vs. wt% SiO_2 for samples from Holes 786A and 786B analyzed at the University of New England. the discriminant line between tholeiitic (TH) and calc-alkaline (CA) types is from Miyashiro (1974). Symbols are as in Figures 3 and 4.

CONCLUSIONS

The igneous basement at Site 786 represents the flanks of a complex, polygenetic volcanic structure of mostly middle Eocene age, but also contains units of Oligocene and Miocene-age (see Mitchell et al., this volume).

Many different lithologies are present, including multiple dikes, pillow lavas, hyaloclastite and lithic-rich breccias, lava flows, and fine-grained sedimentary intervals.

Eight major igneous types are recognized: high-Ca, intermediate-Ca and low-Ca boninites, intermediate-Ca and low-Ca bronzite andesites, andesite, dacite and rhyolite. The bulk chemistry, and in particular the Ca content of the boninite types, overlaps the range of Ca contents previously described world-wide for boninite compositions.

At least in part, this stratigraphy (and chemistry) represents that seen in the upper portions of supra-subduction zone ophiolites. Many equivalent rock types and lithologies are present on the island of Chichijima, the type boninite locality.

The major-element chemistry of this igneous basement is also diverse and complex in detail. A variety of boninites and bronzite andesites, together with silicic rocks such as dacites and rhyolites, are present. We show that these rocks are not simply related to each other by fractional crystallization processes, but that multiple upper mantle sources must have been involved. These sources clearly were highly refractory and probably harzburgitic in nature.

There is a clear geochemical distinction between the igneous rocks presently forming the Bonin forearc basement high and the middle Eocene-to- Pleistocene ash sequences preserved in sediments overlying this basement. An intrinsically more fertile upper mantle source must have been tapped during the genesis of the arc magmas from which the ashes were derived.

ACKNOWLEDGMENTS

R.J.A. and S.v.d.L. express gratitude to USSAC for their logistic support, and for providing funds for essential analytical costs. Other analytical expenses have been supported by Australian Research Council Grant A39030242 to R.J.A., J.A.P., and B.J.M. were supported by a NERC (U.K.) ODP Special Topics research grant (GR3/416). We all recognize the major contributions of Patty Fryer, Laura Stokking, and other shipboard scientists, marine technicians, and the crew of the *JOIDES Resolution* to the success of drilling efforts at Site 786. A. J. Crawford and M.F.J. Flower provided constructive criticism of an early version of the manuscript.

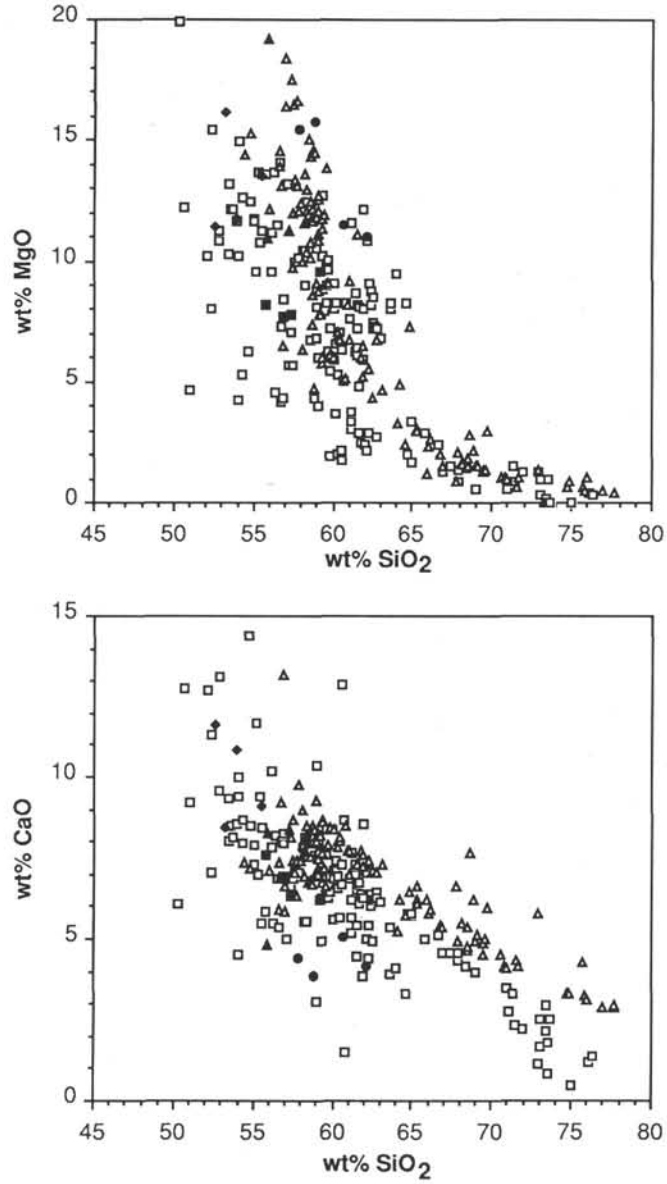

Figure 6. Comparison of the Site 786 igneous basement with the type boninites from Chichijima (Umino, 1986), and other type boninitic suites (high-Ca, low-Ca type 1, low-Ca type 2, and low Ca-type 3) from Crawford (1989), in terms of wt% MgO and wt% CaO vs. wt% SiO_2. Symbols are as in Figures 3 and 4.

REFERENCES

Bloomer, S. H., Hawkins, J. W., 1987. Petrology and geochemistry of boninite series volcanic rocks from the Mariana Trench. *Contrib. Mineral. Petrol.*, 97:361–377.

Cameron, W. E., 1989. Contrasting boninite-tholeiite associations from New Caledonia. *In* Crawford A. J. (Ed.), *Boninites:* London (Unwin Hyman), 314–338.

Crawford, A. J. (Ed.), 1989. *Boninites:* London (Unwin Hyman).

Crawford, A. J., Falloon, J. J., and Green, D. H., 1989. Classification, petrogenesis and tectonic setting of boninites. *In* Crawford, A. J. (Ed.), *Boninites:* London (Unwin Hyman), 1–49.

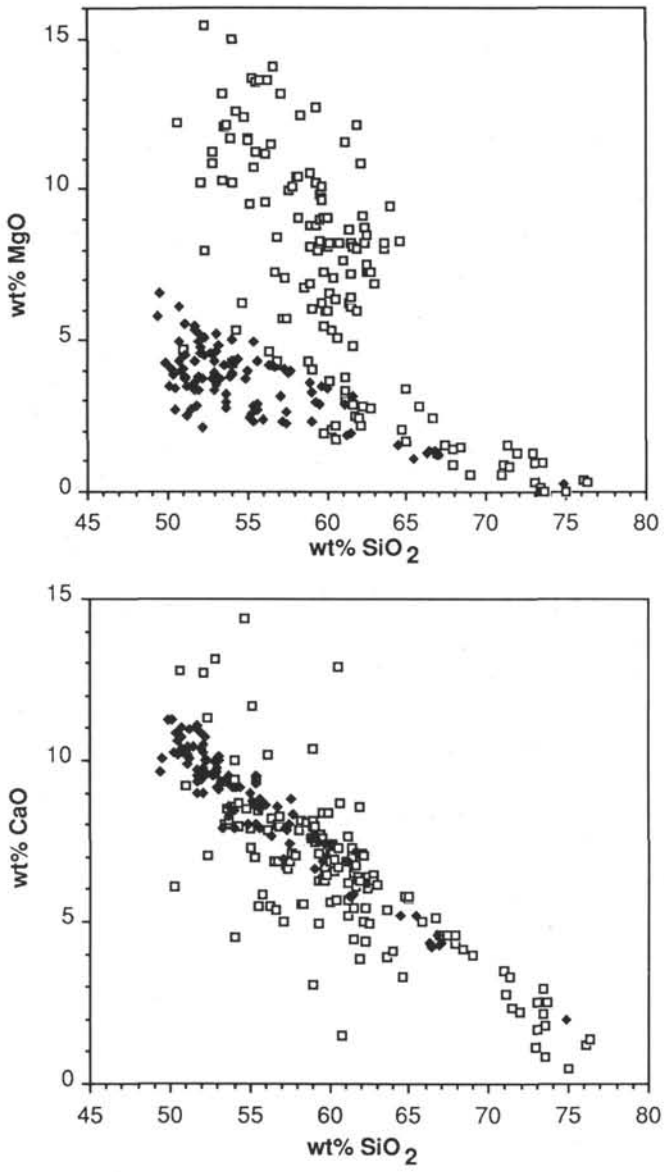

Figure 7. Comparison of the Site 786 igneous basement compositions with the representative (tholeiitic and calc-alkaline), subaerial island arc volcanic suite of Hakone, Japan. Symbols are as in Figures 3 and 4.

Fryer, P., Taylor, B., Langmuir, C. H., and Hochstaedter, A. G., 1990. Petrology and geochemistry of lavas from the Sumisu and Torishima backarc rifts. *Earth Planet. Sci. Lett.,* 100:161–178.

Hickey, R. L., Frey, F. A., 1982. Geochemical characteristics of boninite series volcanics: implications for their source. *Geochim. Cosmochim. Acta,* 46:2099–2115.

Hickey-Vargas, R., 1989. Boninites and tholeiites from DSDP Site 458, Mariana forearc. *In* Crawford, A. J. (Ed.), *Boninites:* London (Unwin Hyman), 339–356.

Honza, E., Tamaki, K., 1985. The Bonin Arc. *In* Nairn, A.E.M, and Uyeda, S. (Eds.), *The Ocean Basins and Margins* (Vol. 7): *The Pacific Ocean:* New York (Plenum), 459–502.

Jaques, A. L., Green, D. H., 1980. Anhydrous melting of peridotite at 0–15 Kb pressure and the genesis of tholeiitic basalts. *Contrib. Mineral. Petrol.,* 73:287–310.

Klaus, A., Taylor, B., in press. Submarine canyon development in the Izu-Bonin Forearc: a SEAMARC II and seismic survey of Aoga Shima Canyon. *Mar. Geophys. Res.*

Miyashiro, A., 1974. Volcanic rock series in island arcs and active continental margins. *Am. J. Sci.,* 274:321–355.

Norrish, K., and Hutton, J. T., 1969. An accurate X-ray spectrographic method for the analysis of a wide range of geological samples. *Geochim.Cosmochim. Acta,* 33:431–453.

Pearce, J. A., Lippard, S. J., and Roberts, S., 1984. Characteristics and tectonic significance of supra-subduction zone ophiolites. *In* Kokelaar, B. P., and Howelle, M. I. (Eds.), *Margin Basin Geology.* Geol. Soc. Spec. Publ. London, 16:77–94.

Pearce, T. H., 1968. A contribution to the theory of variation diagrams. *Contrib. Mineral. Petrol.,* 19:142–157.

Petersen, J., 1891. Der boninit von Peel Island. *Jahrb. Hamburg. Wiss. Anst.,* 8:30.

Reagan, M. K., Meijer, A., 1984. Geology and geochemistry of early arc volcanic rocks from Guam. *Geol. Soc. Am. Bull.,* 95:701–713.

Shipboard Scientific Party, 1990a. Site 782. *In* Fryer, P., Pearce, J. A., Stokking, L. B., et al., *Proc. ODP, Init. Repts.,* 125: College Station, TX (Ocean Drilling Program), 197–252.

———, 1990b. Site 786. *In* Fryer, P., Pearce, J. A., Stokking, L. B., et al., *Proc. ODP, Init. Repts.,* 125: College Station, TX (Ocean Drilling Program), 313–363.

———, 1990c. Site 793. *In* Taylor, B., Fujioka, K., et al., *Proc. ODP, Init. Repts,* 126: College Station, TX (Ocean Drilling Program), 315–403.

Shiraki, K., Kuroda, N., Urano, H., and Maruyama, S., 1980. Clinoenstatite in boninites from the Bonin Islands, Japan. *Nature,* 285:31–32.

Stanley, C. R., Russell, J. K., 1989. Pearce-plot: a turbo-pascal program for the analysis of rock compositions with Pearce element ratio diagrams. *Comput. Geosci.,* 15:905–926.

Sun, S. S., Nesbitt, R. W., 1978. Geochemical regularities and genetic significance of ophiolitic basalts. *Geology,* 6:689–693.

Umino, S., 1985. Volcanic geology of Chichijima, the Bonin Islands (Ogasawara Islands). *J. Geol. Soc. Jpn.,* 91:505–523.

———, 1986. Geological and petrological study of boninites and related rocks from Chichijima, Bonin Islands [Ph.D. thesis]. Univ. of Tokyo.

Wood, D. A., Marsch, N. G., Tarney, J., Joron, J. L., Fryer, P., and Treuil, M., 1981. Geochemistry of igneous rocks recovered from a transect across the Mariana Trough, arc, fore-arc and trench. Sites 453 through 461, DSDP Leg 60. *In* Hussong, D. M., Uyeda, S., et al., *Init. Repts. DSDP,* 60: Washington (U.S. Govt. Printing Office), 611–646.

Date of initial receipt: 1 October 1990
Date of acceptance: 8 August 1991
Ms 125B-137

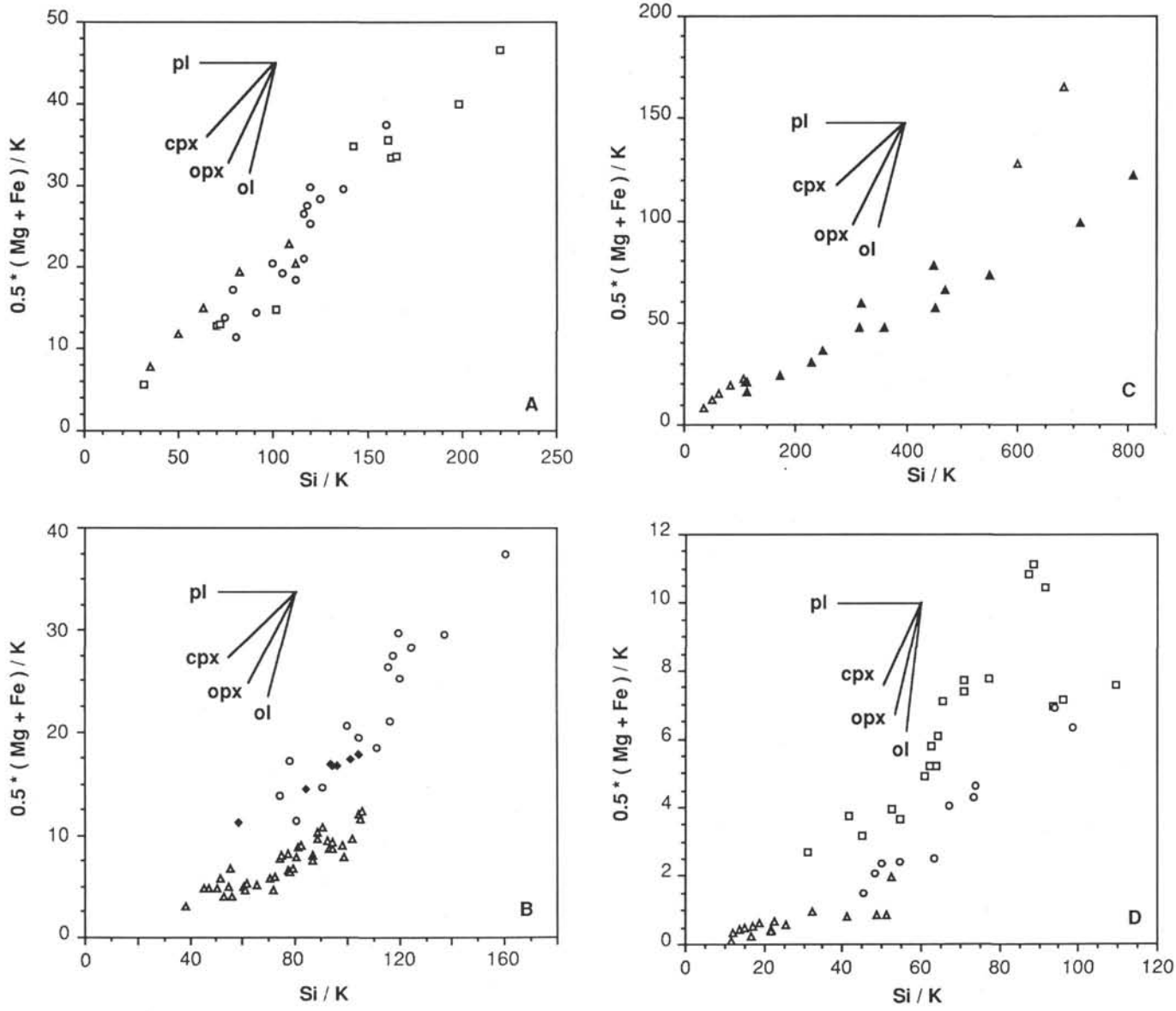

Figure 8. Selected phase discrimination diagrams after Pearce (1968) and Stanley and Russell (1989) for different chemical groups. The slopes of the vectors indicate the effects of specific phase subtraction or addition. The abbreviations are as follows: pl, plagioclase; cpx, clinopyroxene; opx, orthopyroxene; ol, olivine. In 8C and 8D the curved line through the filled diamonds is the progressive equilibrium melting curve from Jaques and Green (1980) for the Tinaquillo peridotite at 10 kbar, with numbers 11 to 40 indicating the percentage of partial melt. In 8E a representative K-alteration vector is drawn through the spread of LCBrzA compositions. The arrowed lines in 8H indicate the effects of fractional crystallization and crystal accumulation of olivine (ol), orthopyroxene (opx), clinopyroxene (cpx), and plagioclase (pl). In 8I and 8J representative K-alteration vectors are drawn through the spread of LCBrzA and R compositions, respectively. The curved vector labeled sp-mt in 8K represents the variable effect of early chrome spinel-late magnetite fractionation. Symbols are as in Figures 3 and 4.

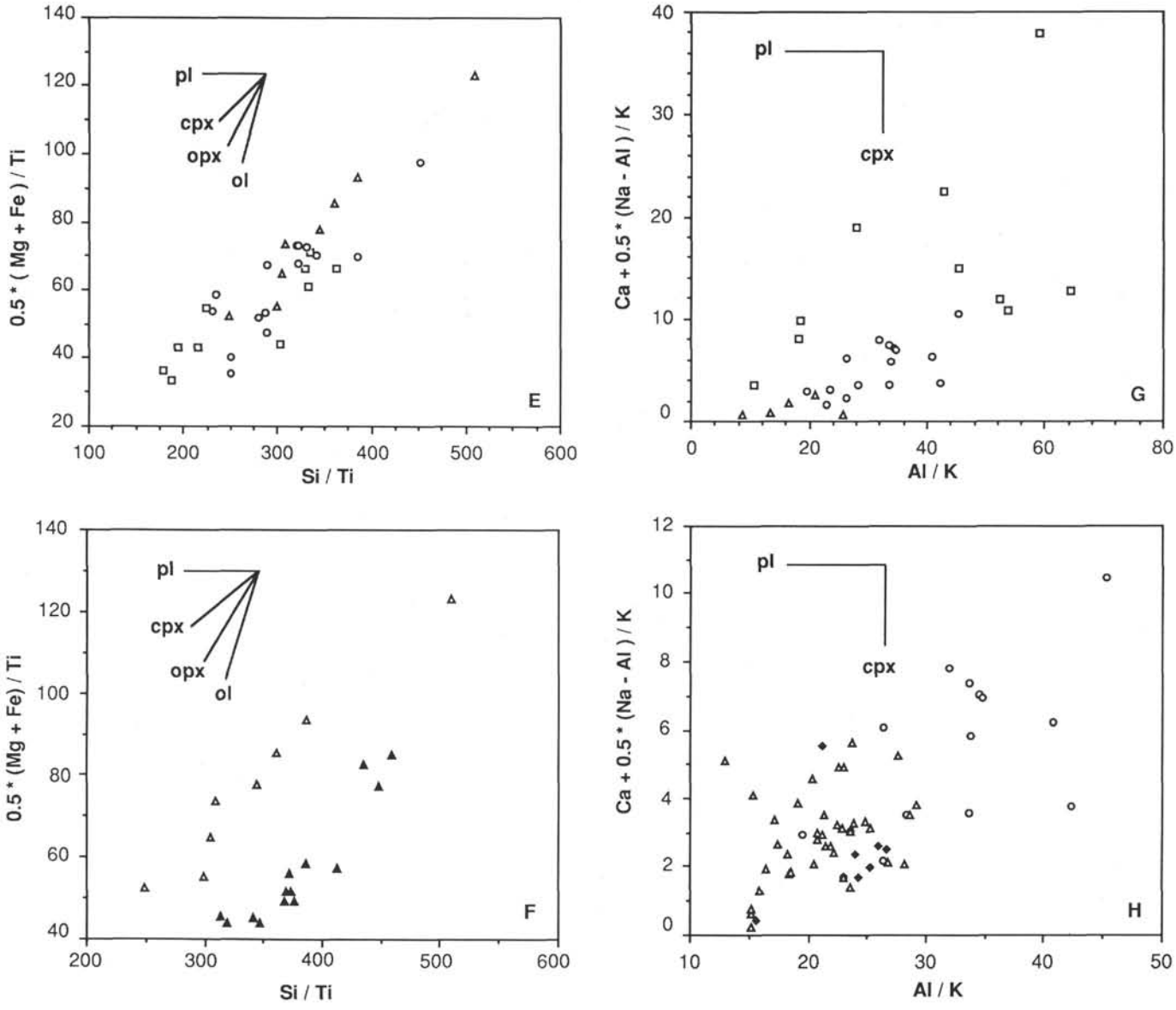

Figure 8 (continued).

Table 5. Summary of lithological occurrences, mineralogical features, and chemical characteristics of the different groups encountered.

	Name	Lithological Occurrence
Group	Chemical Features	Summary of Phenocryst Assemblage
1	High-Ca boninite high-CaO low-intermediate SiO_2 low-intermediate Al_2O_3 intermediate MgO	Dikes, sills 3%–5% euhedral altered olivine trace euhedral orthopyroxene 1%–3% euhedral-corroded clinopyroxene trace plagioclase trace dark-red Cr spinel glomerocrysts of opx + cpx + trace plagioclase
2	Intermediate-Ca boninite intermediate-CaO low-intermediate SiO_2 high-MgO	Flows, dikes, breccia 1%–5% euhedral altered olivine 5%–10% euhedral orthopyroxene 2%–4% euhedral-corroded clinopyroxene 0%–10% euhedral-corroded plagioclase trace Cr spinel
3	Low-Ca boninite low-CaO intermediate SiO_2 high-MgO low-Al_2O_3	Pillow lavas, breccia 5% euhedral fresh to altered olivine 2%–5% euhedral, fresh to altered orthopyroxene 0-trace clinopyroxene trace Cr spinel
4	Intermediate-Ca bronzite andesite intermediate-CaO intermediate-SiO_2 intermediate-MgO low-Al_2O_3	Dikes, lava, breccia 0%–1% altered olivine 6%–20% euhedral orthopyroxene 3%–10% euhedral clinopyroxene 5%–15% euhedral-resorbed plagioclase 0-trace Cr spinel
5	Low-Ca bronzite andesite low-CaO intermediate SiO_2 high-MgO low-Al_2O_3	Dikes, pillow lavas 0%–5% altered olivine 0%–20% altered orthopyroxene trace clinopyroxene trace resorbed plagioclase trace Cr-spinel
6	Andesite intermediate-CaO intermediate-SiO_2 low-MgO high to very high-Al_2O_3	Dikes, breccia 0-trace orthopyroxene 1%–3% euhedral clinopyroxene 3%–5% euhedral plagioclase some phenocryst magnetite
7	Dacite intermediate-CaO intermediate-SiO_2 low-MgO high-Al_2O_3	Dikes, flows, breccia 0%–5% euhedral-corroded orthopyroxene trace-2% euhedral-resorbed clinopyroxene 3%–10% plagioclase phenocryst magnetite
8	Rhyolite low-CaO high-SiO_2 low-MgO low-Al_2O_3	Dikes, flows 0-trace euhedral orthopyroxene 0-trace euhedral-anhedral clinopyroxene trace-3% resorbed plagioclase trace quartz phenocryst magnetite common
9	Mixed group	Clasts in breccia

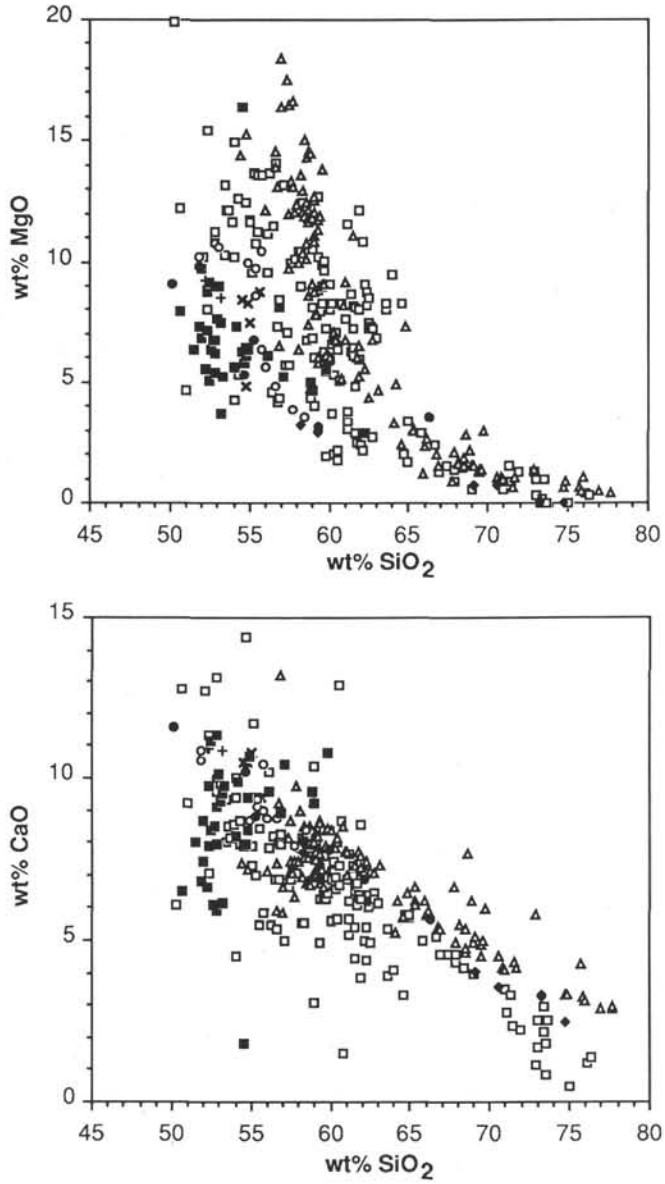

Figure 9. Comparison of the Site 786 igneous basement lithologies with other Eocene-Oligocene rock suites located in Bonin-Mariana forearc settings. Data from Shipboard Scientific Party (1990c), Wood et al. (1981), Reagan and Jeijer (1984), and Umino (1986). Symbols are as in Figures 3 and 4.

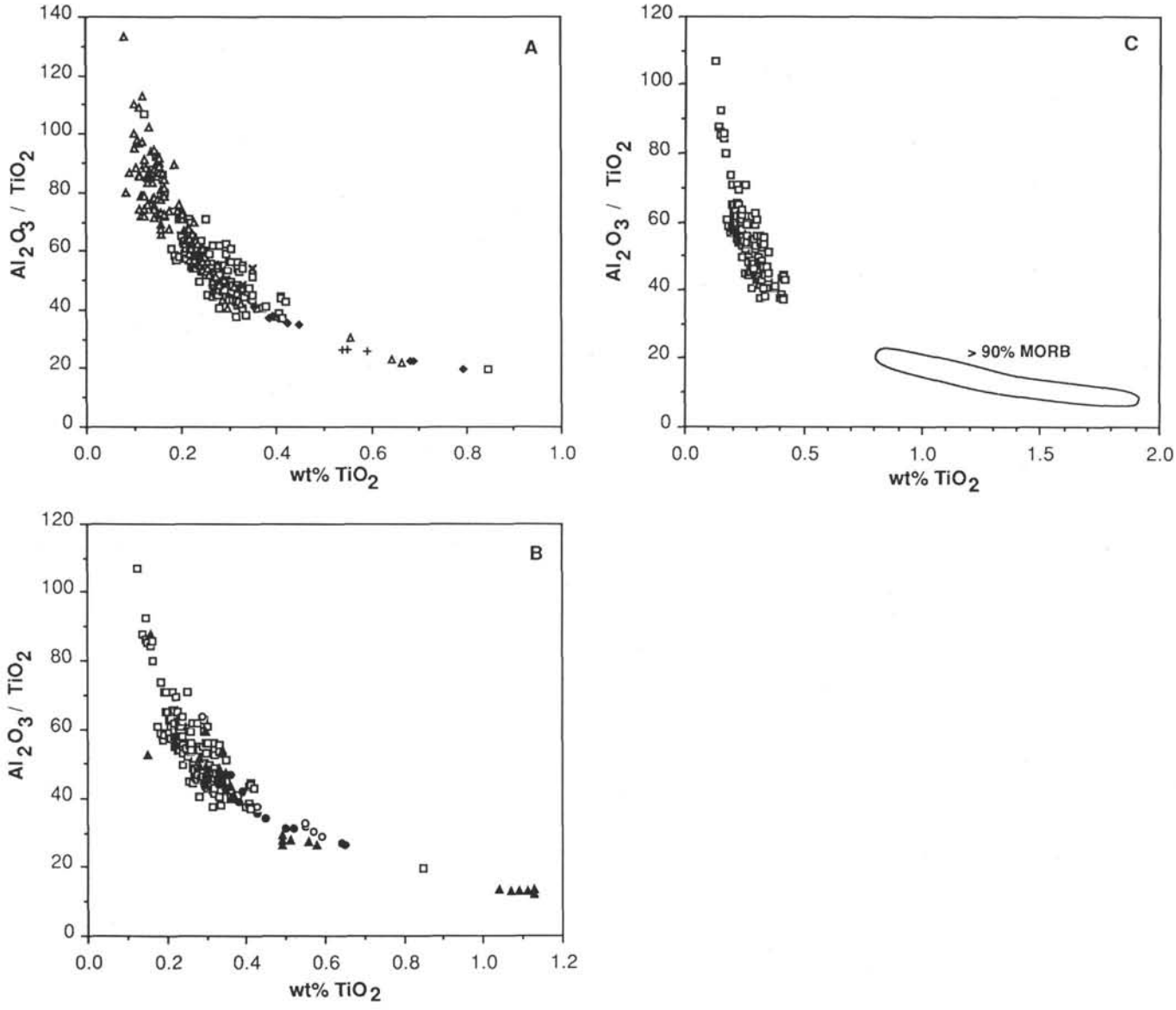

Figure 10. Variation of refractory lithophile oxides based on diagrams from Sun and Nesbitt (19878) and Hickey and Frey (1982), and data from references cited in the text. Symbols are as in Figures 3 and 4.

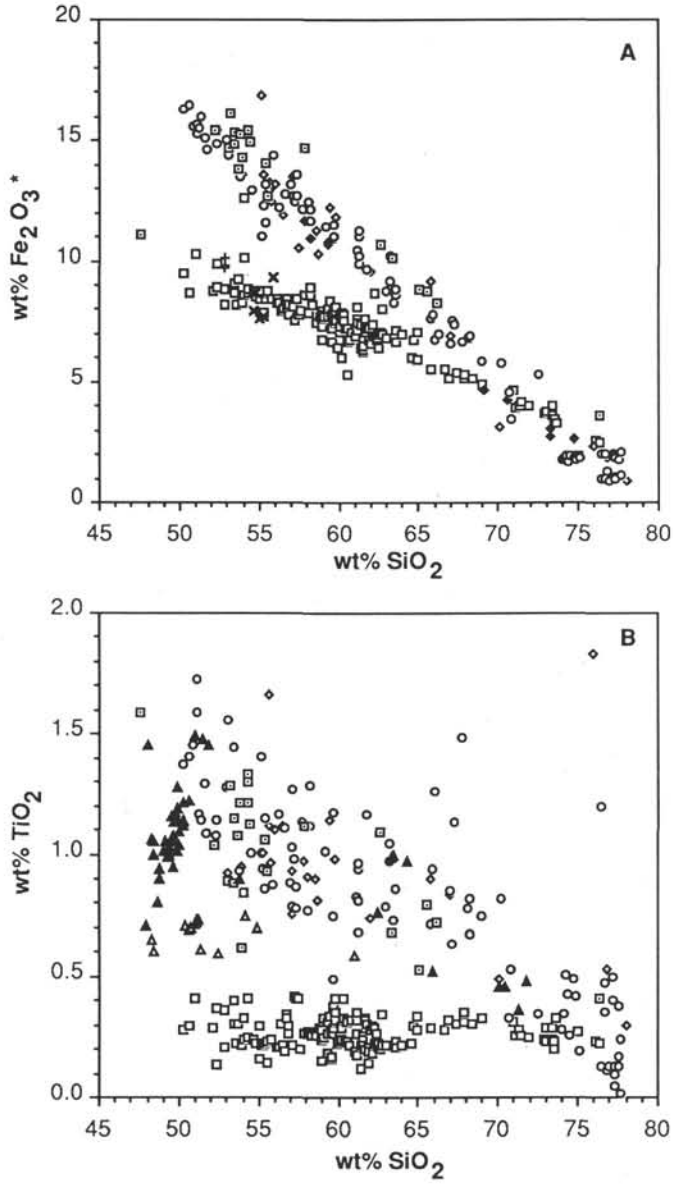

Figure 11. Selected geochemical comparison of sites on the forearc basement high and Bonin Trough with Eocene-Pleistocene ashes overlying these sites (see Arculus and Bloomfield, this volume). Data for the bonin subaerial arc and backarc rift are from Fryer et al. (1990). Symbols are as in Figures 3 and 4.